27

MEDSUDMED - TECHNICAL DOCUMENTS

Report of the MedSudMed-06 oceanographic survey, Libyan continental shelf (south-central Mediterranean Sea) 12-24 August 2006

MEDSUDMED

FAO FIAT PANIS

Cover photograph:
Ichthyoplankton sampling net. Courtesy of Jerina Kolitari

ASSESSMENT AND MONITORING OF THE
FISHERY RESOURCES AND THE ECOSYSTEMS
IN THE STRAITS OF SICILY

GCP/RER/010/ITA
GDCP/INT/010/ITA

MedSudMed

Report of the MedSudMed-06 Oceanographic Survey, Libyan continental shelf (south-central Mediterranean Sea) 12 – 24 August 2006

MedSudMed Technical Documents
GCP/RER/010/ITA/MSM-TD 27

Rome (Italy) August 2012

The conclusions and recommendations given in this and in other documents in the *Assessment and Monitoring of the Fishery Resources and Ecosystems in the Straits of Sicily* Project series are those considered appropriate at the time of preparation. They may be modified in the light of further knowledge gained in subsequent stages of the Project. The designations employed and the presentation of material in this publication do not imply the expression of any opinion on the part of FAO or MiPAAF or Regione Siciliana concerning the legal status of any country, territory, city or area, or concerning the determination of its frontiers or boundaries.

Preface

The Regional Project "Assessment and Monitoring of the Fishery Resources and the Ecosystems in the Straits of Sicily" (MedSudMed) is executed by the Food and Agriculture Organization of the United Nations (FAO) and funded by the Italian Ministry of Agriculture, Food and Forestry Policies (MiPAAF). The Italian Regione Siciliana funded a project aimed at strengthening MedSudMed's effectiveness on issues related to demersal resources, namely crustaceans, for 18 months, starting from May 2011.

MedSudMed promotes scientific cooperation between research institutions of the four participating countries (Italy, Libya, Malta and Tunisia), for the continuous and dynamic assessment and monitoring of the status of the fisheries resources and the ecosystems in this area of the Mediterranean Sea.

Research activities and training are supported to increase and use knowledge on fisheries ecology and ecosystems, and to create a regional network of expertise. Particular attention is given to the technical coordination of the research activities between the countries, which should contribute to the implementation of the Ecosystem Approach to Fisheries. Consideration is also given to the development of an appropriate tool for the management and processing of data related to fisheries and their ecosystems.

FAO MedSudMed Project
FAO-FIRF Room C350-353
Viale delle Terme di Caracalla
00153 Rome, Italy

TEL: +39 06 570 54492/56092
FAX:+39 06 570 55188
e-mail: faomedsudmed@faomedsudmed.org
URL: http://www.faomedsudmed.org

GCP/RER/010/ITA Publications

The MedSudMed Project publications are issued as series of Technical Documents (GCP/RER/010/ITA/MSM-TD-00) and Scientific Reports (GCP/RER/010/ITA/MSM/SR-00) related to meetings, missions and research organized by or conducted within the framework of the Project.

Comments on this document would be welcomed and should be sent to the Project headquarters:

FAO MedSudMed Project
FAO-FIRF Room C350-353
Viale delle Terme di Caracalla
00153 Rome
Italy
medsudmed@fao.org

For bibliographic purposes this document
should be cited as follows:

Bonanno, A., Zgozi, S., Bahri, T. (eds) 2008. Report of the MedSudMed-06 Oceanographic Survey, Libyan continental shelf (south-central Mediterranean Sea) 12 – 24 August 2006. GCP/RER/010/ITA/MSM-TD. *MedSudMed Technical Documents*, 27: 53 pp.

Preparation of this document

Oceanographic surveys are probably the most important source of data to investigate the ecology, abundance and spatial distribution of small pelagic fish species, and to detect possible influence of environmental factors on their abundance and distribution. The experts of the countries participating in the FAO Project MedSudMed (*Assessment and Monitoring of the fisheries Resources and the Ecosystems in the Straits of Sicily*) during the MedSudMed Expert Consultation on Small Pelagic Fishes: Stock Identification and Oceanographic Processes Influencing their Abundance and Distribution (Tunisia, October 2003) deemed necessary to expand the area covered by oceanographic surveys and investigate areas where little or outdated information on eggs and larvae was available.

This document is the final version of the report of the MedSudMed Oceanographic Survey carried out in Libyan waters from 12 to 24 August 2006 on board of the R/U Urania. The document presents also the results of the processing of the data collected during the survey. The survey was organised in the framework of the MedSudMed Project in cooperation with the Istituto per l'Ambiente Marino Costiero (IAMC-CNR) of Mazara del Vallo (Italy) and the Marine Biology Research Centre (MBRC) of Tajura (Libya). Other collaborating research institutes involved in the survey and in the data processing are: i) VNIRO, Fishery Acoustic Laboratory, Moscow, Russia; ii) ISMAR-CNR, Istituto di scienze marine, Sezione di Oceanografia Fisica, La Spezia, Italy; iii) Istituto Nazionale di Geofisica e Vulcanologia, La Spezia, Italy; and iv) IAMC – CNR of Messina, Italy. The outcomes of the survey and data processing described in this report contributed to the publication of MedSudMed identification sheets for early life sages of bony fish (MedSudMed Technical document No. 18[1] http://www.faomedsudmed.org/pdf/publications/TD18.pdf).

This report is one of outcomes of the MedSudMed Project component on "Small Pelagic Fish: Stock Identification and Oceanographic Processes Influencing their abundance and distribution". This report is primarily for scientists of the south-central Mediterranean Sea; it can also be of interest for students and professional of fisheries research and management in the Mediterranean Sea region. It is believed to be a contribution to better knowledge on the distribution and abundance of small pelagic fish eggs and larvae in an area not fully investigated.

Scientists who contributed in the data processing, report writing and training are (alphabetic order): Grazia Maria Armeri, Salvatore Aronica, Filippo Azzaro, Gualtiero Basilone, Sergio Bonomo, Mireno Borghini, Giuseppa Buscaino, Luca Caruana, Angela Cuttitta, Osama Drebika, Akram El Turki, Ignazio Fontana, Gianpietro Gasparini, Giovanni Giacalone, Hisham Ghmati, Rosario Grammauta, Mohamed Hamza, Marcella Leonardi, Salvatore Mazzola, Bernardo Patti, Carlo Patti, Sergey Popov, Abdul Bari Ramadan, Luca Saporito, Mostapha Talha.

[1] FAO MedSudMed 2011. Identification sheets of early life stages of bony fish. Western Libya, Summer 2006. GCP/RER/010/ITA/MSM-18 (MedSudMed Technical Documents n°18). 2011. 251pp.

Acknowledgements

The Libyan Authorities, through the General Authority of Marine Wealth, are gratefully acknowledged for their support. Mr. Nurredin Essarbout (MBRC, Libya) and Mr. Salvatore Mazzola (IAMC-CNR, Italy) are warmly thanked for the efforts spent and the support provided in the organization of all activities and for making this work possible. Mr. Emanuele Gentile, Master of the R/V Urania and all his crew are thanked for their work. Sergio Bonomo, Marina Locritani, Hisham Ghmati and Vincenzo Pernice are acknowledged for providing photos for this report.

Report of the MedSudMed-06 Oceanographic Survey, Libyan continental shelf (south-central Mediterranean Sea) 12 – 24 August 2006.
MedSudMed Technical Documents. No. 27. GCP/RER/ITA/MSM-TD-27, Rome, 2011: 53 pp.

ABSTRACT

This document is the final version of the report of the MedSudMed Oceanographic Survey carried out in Libyan waters from 12 to 24 August 2006 on board of the R/V Urania. The document presents also the results of the processing of the data collected during the survey. The survey was carried out under the cooperative framework promoted by the FAO Project MedSudMed (Assessment and Monitoring of the Fishery Resources and the Ecosystems in the Straits of Sicily). The main objective of the survey was to collect information on areas of concentration of eggs and larvae of small pelagic fish species and relate them to the mesoscale physical aspects characterizing the area. During the survey, advantage was also taken to collect sediments and water samples to update and/or complement existing information on bottom types and study the chemical-physical properties of the water masses. The results were expected to complement information available in the rest of the MedSudMed area, where hypothesis were drawn on the transport and retention processes of small pelagic fish eggs. The main target species for the ichthyoplankton study were anchovy (*Engraulis encrasicolus*) and round sardine (*Sardinella aurita*). An overall description of the sampling scheme, of the area explored and of the methods adopted is provided. The distribution and abundance of eggs and larvae of *E. encrasicolus* and *S. aurita* in Libyan waters is described, as well as the composition and abundance of phytoplankton. The main oceanographic characteristics, including water mass circulation, in the western Libyan waters are also illustrated. A description of the trophic status of the waters is also provided taking into account nutrients and suspended matter. A description of the content of trace elements and nutrients in the water column complete the information provided in this report.

Table of Contents

List of Figures

List of Tables

Acronyms

IAMC-CNR: Istituto per l'Ambiente Marino Costiero– Consiglio Nazionale delle Ricerche

UOD = Unità Operativa Distaccata (Separate Operative Unit)

MBRC: Marine Biology Research Centre, Tripoli, Libya

VNIRO: Fishery Acoustic Laboratory, Moscow, Russia

ISMAR-CNR: Istituto di Scienze Marine, Sezione di Oceanografia Fisica, La Spezia, Italy

CTD: Conductivity, temperature and depth instrument

ADCP: Acoustic Doppler current profiler

1 Introduction

The regional assessment of small pelagic fish stocks and the study of the spatial distribution of the different life stages in relation to environmental parameters is one of the research activities endorsed by the MedsudMed Coordination Committee. This activity is developed in the framework of the MedSudMed Project component on "Small Pelagic Fish: Stock Identification and Oceanographic Processes Influencing their abundance and distribution".

For the scientific cooperation, for the standardization sake and in order to conduct activities at regional scale, the MedSudMed Project has put much effort in the support of those institutes who requested strengthening their capacity building. In this line, the Project supported the organization of an oceanographic and ichtyoplankton survey in cooperation between the Marine Biology Research Centre (MBRC) of Tajura, Libya and the Istituto per l'Ambiente Marino Costiero (IAMC-CNR) of Mazara del Vallo, Italy, in order to collect data in areas where little or outdated information was available. Other Institutes participated in the survey in quality as partners of the IAMC-CNR for their expertise on specific topics. The oceanographic survey MedSudMed-06 was conducted on board the Italian R/V "Urania" from 12 to 24 August 2006 in the western part of the Libyan waters and was the first one of its kind since 1973.

The main scope of the data collection was to locate the areas of major concentration of eggs and larvae of small pelagic fish species and relate them to the mesoscale physical structures characterizing the area. The results were expected to complement information available in the rest of the MedSudMed area, where hypothesis were drawn on the transport and retention processes of small pelagic fish eggs. Considering the reproduction period of small pelagic fish in this area, the main target species were anchovy (*Engraulis encrasicolus*) and round sardinella (*Sardinella aurita*).

Besides the main scientific target of the survey, advantage was also taken to collect sediments and water samples to update and/or complement existing information on bottom types and study the chemical-physical properties of the water, such as concentration of nutrients in the water column and trace elements concentration in located spots (i.e. in front of the main cities of the study area). The survey was also the occasion to provide on-the-job training and reinforce cooperation relationships between the Institutes.

Prior to the survey, it was agreed that data and samples would be processed jointly by the different participating Institutes and, whenever required, training courses would be organized in laboratory. As a result, six training courses were organized in order to process the data and draft technical reports that were used as basic material for this document.

This document gives an overview of the work carried out at sea and describes the main findings related to different topics (ichtyoplankton, oceanography, sediments, phytoplankton, organic matters, nutrients, trace elements, meteorology). The aim is to provide an overview of the activities carried out and the information retrieved from them.

2 Basic observational strategy

The sampling design was based on the one adopted in 1974 (Zorgani, 1982), with collection of samples at least in the same sampling stations than in 1974. Samples were not collected at less than 3 nm from the coast and were duplicated in such way as to provide MBRC with a set of samples at the end of the survey. In total, the following samples were collected:

- 52 ichtyoplankton samples
- 120 anchovy larvae preserved individually in liquid nitrogen
- 40 Box Corer samples (samples in PVC tubes)
- 41 Sediments samples (samples in plastic bags)
- 52 CTD casts and ADCP profiles
- 3 waters samples (trace elements)
- 14 water samples (nutrients and micro-algae)
- Continuous acoustic data
- Continuous sodar data
- Meteorological data.

The study area is shown on Figure 1.

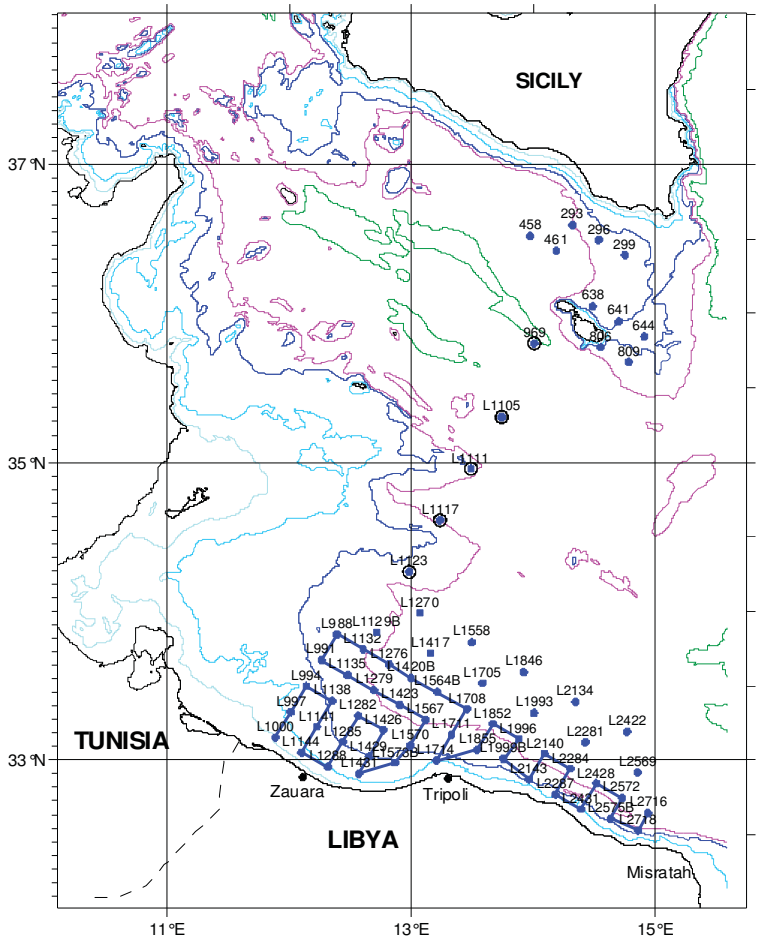

Figure 1. Position of stations with CTD, ADCP and Bongo40 during the MedSudMed-06 survey on board the R/V Urania. No sample was collected with the Bongo 40 in stations with black circle. The blue line represents the track of the vessel along which data were collected with the Biosonics DTX.

3 Ichtyoplankton

3.1 Biological sampling

3.1.1 Material and method

a. Samples collection

Biological samples were collected by means a Bongo 40 net with a 200 µm mesh size for both sizes of the frame. Flowmeters were used in each net (General Oceanics, mod. 2030R). A depressor was used during the net hauling to enhance the stability of the nets. The lowering speed of the net was 0.75 m/s and the ascending speed 0.33 m/s. The Bongo40 net hauls described an oblique trajectory from the surface to 100 m depth or to the bottom in areas where depth was less than 100 m, at a constant speed of 2 knots with a cable inclination of about 45 degrees. A total of 52 samples were collected, using a regular sampling grid of 12 nm.

Each collected sample was rapidly analyzed under stereomicroscope and whenever a high number of anchovy larvae was detected, a further sample was collected in order to have a replicate from which anchovy larvae were extracted. A Bongo 60 was meant to be used for the replicates, however, during the collection of the 1st replicate, it was discovered that the Bongo 60 was not appropriate due to the difficulties associated to bad weather conditions, therefore the samples replicates were collected using the Bongo 40. A total of 5 replicates were collected (Figure 2). Samples were fixed immediately after collection and preserved in a 4% buffered formaldehyde seawater solution; the individual larvae were conserved in liquid nitrogen[2].

b. Samples processing

Ichthyoplankton composition was estimated on samples coming from one of the two mouths of the Bongo 40 net. Zooplankton biomass values are expressed as Wet Weight (W.W.) and Dry Weight (D.W.) (mg m^{-3}), according to Lovegrove (1966).

3.1.2 Results

The larvae sorting are reported in the following table which shows that the predominant species was anchovy (*Engraulis encrasicolus*) representing about 51% of the collected larvae and round sardinella (*Sardinella aurita*) with 9.6% of the larvae. Each of the other species represents only a minor fraction of the collected larvae, except the Serranidae family (5.6%), the Gobidae family (3.7%), *Auxis rochei* (2.3%) and the Labridae family (3%).

	Number of Bongo40 stations	Number of Anchovy larvae	% of Anchovy larvae	Number of Sardinella larvae	% of Sardinella larvae	Other larvae	% of Other larvae	Total number of larvae
GSA 21 (Western Libya)	52	1123	51	212	9.6	758	39.4	2202

Among the larval specimens collected in the Libyan waters, a total of 11 Orders, 39 Families, 39 Genera and 40 Species were identified

Figure 3 and Figure 4 show the densities of anchovy eggs and larvae.

[2] These samples could be used in the future for possible biochemical analysis and/or micro otolith reading. They were not analysed for the purpose of this report.

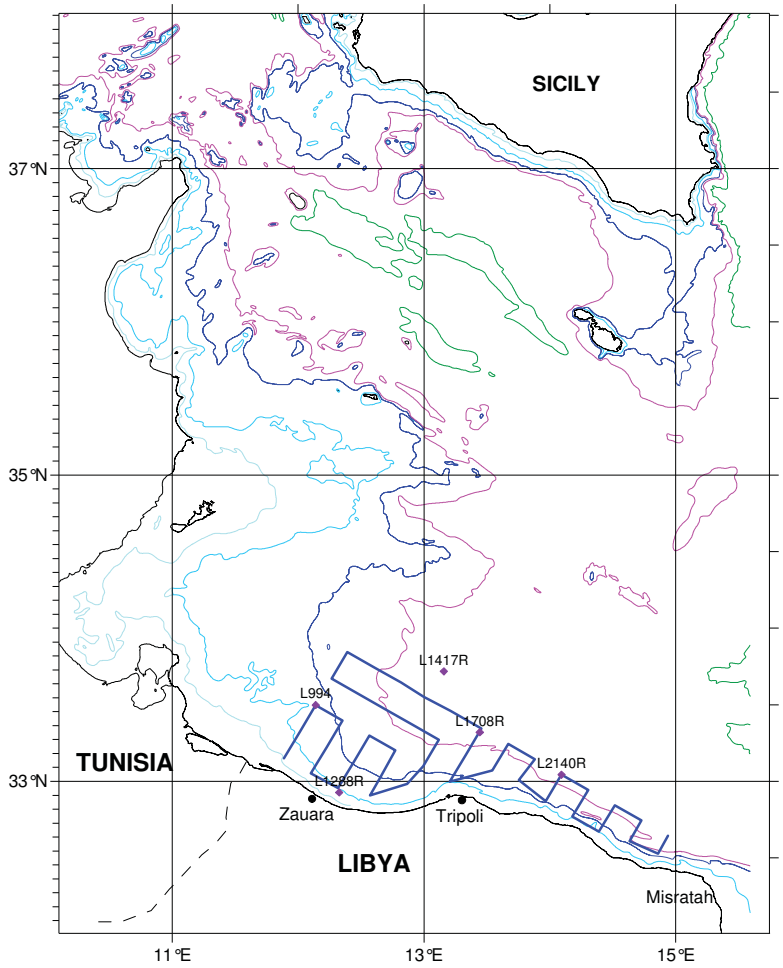

Figure 2. Position of the stations where replicates of Bongo 40 and Bongo 60 were collected.

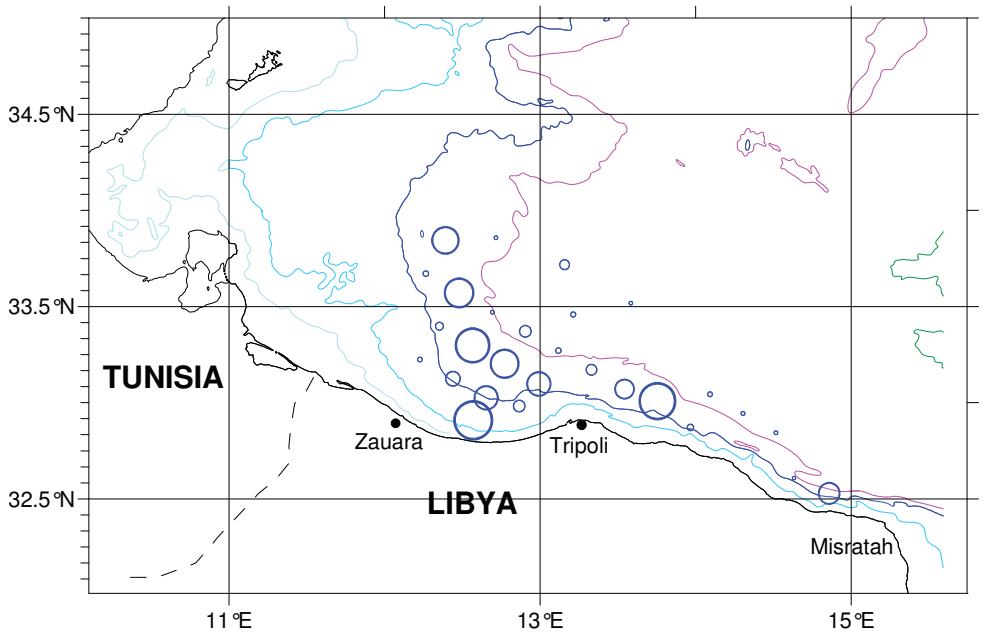

Figure 3. *Engraulis encrasicolus* eggs density; range 0 – 1.38 eggs/m^3.

The area with the highest concentration of anchovy eggs is located in the western part of the surveyed area with high densities in the area characterized by depths of about 150 m. High values of eggs density were also found in more coastal sea areas between Zauara and Tripoli and east of Tripoli. Anchovy larvae were found in almost all the station of the study area but higher densities were located in the western part of the study area. The easternmost area revealed intermediate larvae densities and low densities of eggs.

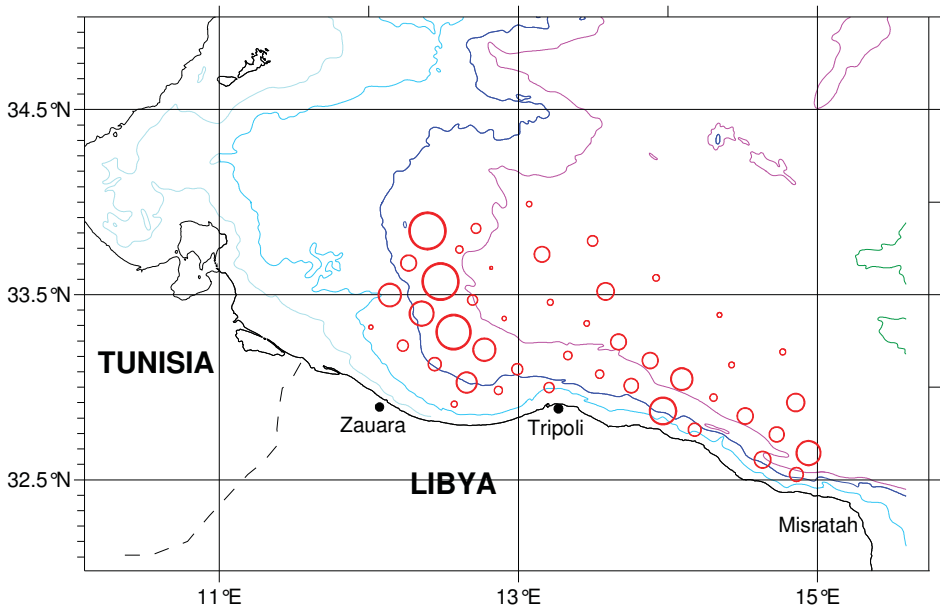

Figure 4. *Engraulis encrasicolus* larvae density; range 0 – 1.81 larvae/m^3.

As above mentioned, all the larvae collected in closer stations to the coast were measured and weighted. Figure 5 shows the mean length of anchovy larvae (symbols proportional to the lengths) superimposed to the densities (larvae/m^3). In the western part the highest larvae densities correspond to the lowest anchovy mean lengths. In the eastern area smaller anchovy larvae lengths were found in more coastal waters.

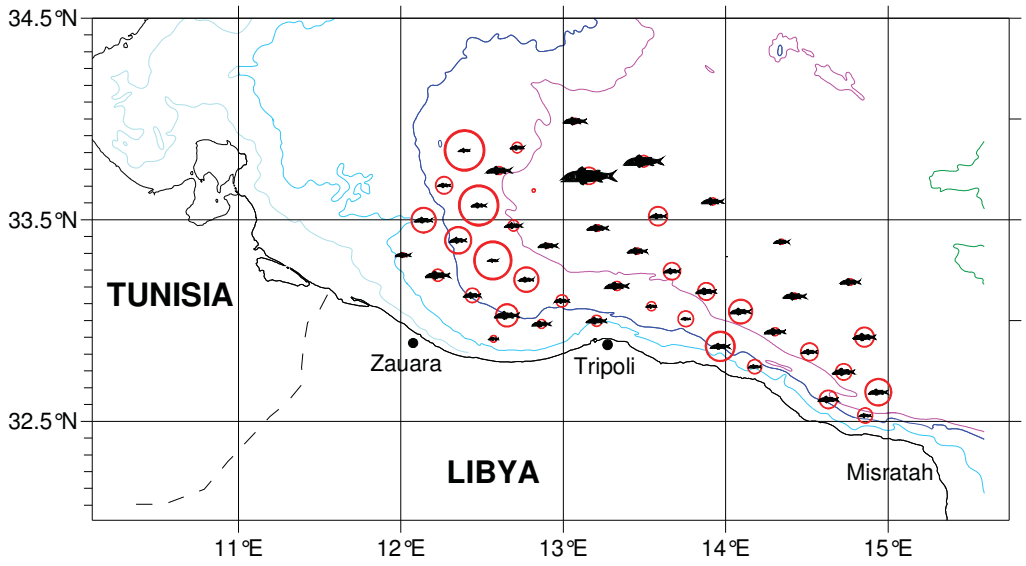

Figure 5. Mean length of *Engraulis encrasicolus* larvae in closer stations to the coast (range 3 – 20 mm). Larvae density is proportional to the radius of red circles (range 0 – 1.81 larvae/m^3).

These findings seem to suggest a different influence of the circulation on the distribution of anchovy eggs and larvae in the western area and in the eastern one. In particular, in the western area, probably characterized by slow sea water masses dynamics, high values of eggs and larvae densities were found in the same stations, except in the coastal area between Zauara and Tripoli where only high eggs density was observed. Furthermore, in these stations anchovy larvae with smaller sizes have been collected.

The eastern area reveals the possible influence of a surface current flowing parallel to the coast. The stations with high eggs density are located east of Tripoli, while anchovy larvae density, as above mentioned, reached intermediate values along almost all the eastern surveyed area. In this part of the Libyan area lower anchovy mean lengths are found in the stations with higher eggs densities but with lower larvae densities. These findings suggest a possible transport process of anchovy spawning products towards the easternmost part of the surveyed area.

Figure 6 shows the distribution of the *Sardinella aurita* larvae densities and length (mean larvae length in each station is proportional to the symbol). The larvae distribution pattern singles out a preference of such species for lower depths. Moreover, higher densities were found in the western area, even though this species was found in fewer stations respect to anchovy. Round sardinella is the main species caught by Libyan fishermen exploiting small pelagic fish. The high larvae densities in the western part of the study area may suggest the preference of this species for lower depths.

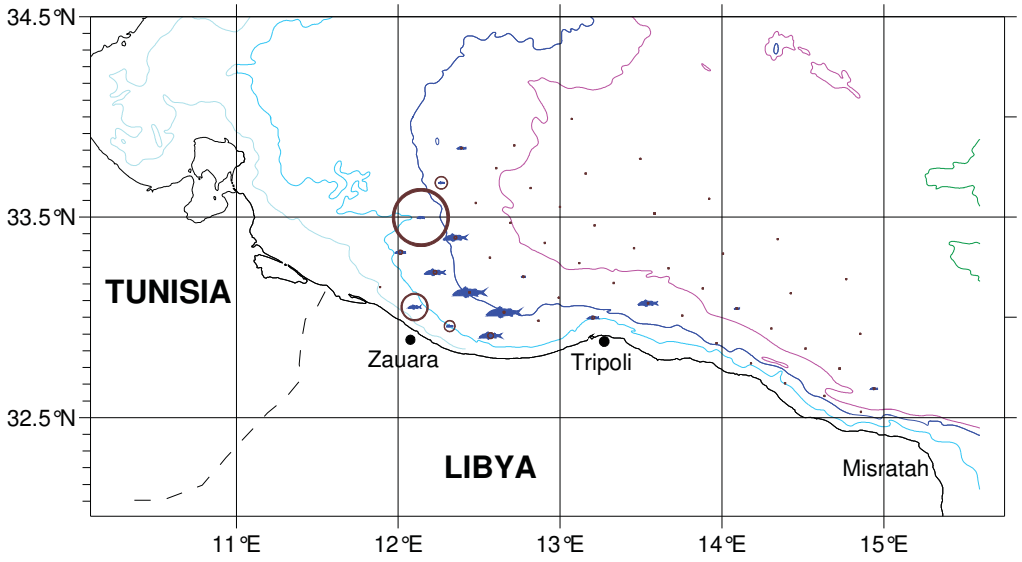

Figure 6. Mean length of *Sardinella aurita* larvae in closer stations to the coast (range 2.8 – 8.6 mm). Larvae density is proportional to the radius of brown circles (range 0 – 1.97 larvae/m^3).

3.2 Acoustic sampling

The main aim of the study was to evaluate the distribution pattern of small organisms such as zooplankton and fish-larvae. As there is no standard procedure to evaluate the biomass of larvae of different fish species, two methods to estimate larval density of the target species were suggested and discussed.

3.2.1 Material and methods

The hydro-acoustic survey conducted on board the R/V Urania included the following stages:

- ✓ installation of equipment on board the vessel and operation test;
- ✓ echo-sounder calibration using the standard sphere method;
- ✓ choice of transects according to vessel time availability and research aims;
- ✓ choice of equipment parameters during the survey;
- ✓ acoustic data acquisition;
- ✓ data processing, echo integration and analysis of results.

a. Installation of equipment

The acoustic data acquisition was carried out with the Biosonics DTX echo-sounder (Figure 7), equipped with two split-beam transducers operating at 208 and 418 kHz. The central unit was in the electronic laboratory of the vessel while both the split-beam transducers were installed on a Biosonics towed body. During the acoustic data acquisition phase, the towed body was put in the sea, about 2.5 m under sea surface, by means of a stainless steel rope tied to a 5-m long bar. In this way both transducers were positioned about 4 m distant from the right-hand side of the vessel and none of them received any backscattering signal from the vessel hull.

A GPS unit, interfaced with the echo-sounder central unit, permitted to acquire speed and position of the vessel during the survey.

Figure 7. Biosonics DTX Echo-sounder with 2 transducers

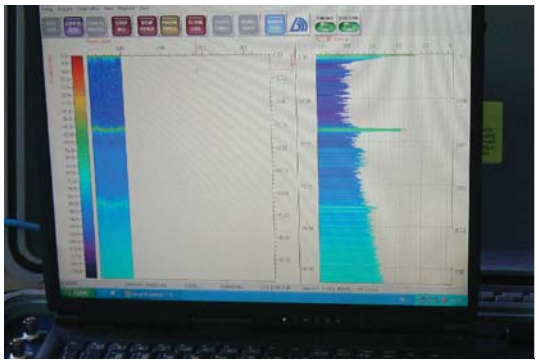

Figure 8. Example of recorded echogram showing the highest backscattering layers corresponding to the surface and to the bottom

b. Calibration of the echo-sounder

The echo-sounder calibration procedure was carried out in Cape Granitola harbor on 9 August 2006. The standard sphere method was adopted to calibrate the echo sounder, with a tungsten sphere with 36 mm diameter and target strength (TS) of –40 dB for the split-beam transducer pulsing at 208 kHz and TS of –43 dB for the split-beam transducer at 418 kHz.

c. Choice of transects according to vessel time availability and research aims

The acoustic data collection was performed along transects between biological stations (see Figure 1). The original idea was to cover the study area along equally-spaced parallel transects, perpendicular to the coastline. Due to bad weather conditions, the survey design was modified; the final cruise track is shown in Figure 1. According to vessel time availability and the main aims of the survey, the acoustic data acquisition started at station L1000 and ended at station L2716 close to Misratah (Figure 1).

d. Choice of equipment parameters during the survey
During the whole echo-survey the pulse duration was set at 1 ms for both frequencies, the pulse rate at 1 s and the emitted power at the maxima values for both transducers. It was also decided to acquire acoustic data in the depth layer 0 – 100 m since the biological samples were collected by the Bongo40 net in the same layer. Moreover, a minimum value for the volume backscattering strength (Sv, dB) was set to -80 dB since the main aim of the acoustic data acquisition was to evaluate the distribution pattern of small organisms like larvae or zooplankton.

e. Acoustic data acquisition
The acoustic device used imposed to reduce the vessel speed at 5-6 knots. Data were continuously collected (day and night), except during the CTD and Bongo stations where the echo-sounder was turned off.

f. Data processing, echo integration and results display
The hydro-acoustic signals were analyzed by means of the post-processing system Echoview ver. 3.50 (SonarData Pty Ltd). The Elementary Sampling Distance Unit (ESDU) of the hydro-acoustic data was 1 nautical mile.

Filtering of noise and extraction of useful signals
The extraction of useful signals from background noise or from other sound-scattering layers is a fundamental aspect to be considered during hydro-acoustic data processing. In the study area a variety of marine organisms, like adult fish, fish-larvae and zooplankton, were contemporarily present and these organisms were registered without distinction by the echo-sounder.

The aim of the study was to evaluate the distribution pattern of small organisms such as zooplankton and fish-larvae, therefore it was important to remove from the hydro-acoustic data the effects of other signals scattered by undesired organisms or air bubbles. In this study the single-frequency method was used because the highest frequency (418 kHz) transducer often acquired noisy echograms. During the post-processing procedure both manual and automatic echoes selection procedures were used. The visual analysis during manual signal selection allowed removing non-biological signals from processed data. These signals were produced by surface bubbles, noise from turbulence, vessel noise and navigation equipment noise. Bubbles are always present near the ocean surface, and may input strong biases in all measurements. In particular, air bubbles contamination may affect measurements in the shallow water layer not deeper than 5-10 m. Only the visual analysis of the echograms allowed both recognizing backscattering signals produced by non-biological sources and removing them from the collected acoustic data by means of the post-processing software.

Operating frequency and choice of depth layers
The output of the post-processing procedure was the estimate of the Nautical Area Scattering Coefficient (*NASC*, m^2/nmi^2) for each ESDU in two different depth layers: 0-40m and 0-80 m. The setting of the integration layers was mainly conditioned by the echo-sounder capability to acquire useful signals along the water column. According to the signal-to-noise ratio measurements, previously made on this instrumentation, acquisition of hydro-acoustic data with the frequency 208 kHz was possible in the range 0-80 m, while data acquisition with the frequency 418 kHz was possible only in the range 0-40 m. Outside the specified ranges the noise level started to exceed zooplankton and/or fish-larvae signals. As correct data acquisition was possible only in a narrow depth range at 418 kHz frequency, no

multifrequency post-processing method was applied and only data collected at 208 kHz were used.

Estimation of larvae density

A standard procedure for larvae biomass estimate is still not defined, as in different sea areas zooplankton and larval organisms may combine in complex assemblages and produce different backscattering signals. Starting from the estimated NASC values for each ESDU, two methods for larvae biomass estimation were applied and discussed for the purpose of this report. The application of both methods depended on ichthyoplankton samples processing (identification of species, number, length and weight of individuals) performed on biological samples.

In both methods the same operations were used for the determination of the fish-larvae NASC ($NASC_L$). The EchoView software allowed removing the "noisy regions" (areas with noise from different sources) from echograms, and to set a "threshold level" for the extraction of the combined zooplankton and fish-larvae NASC ($NASC_M$) from the total NASC. This last step was necessary to exclude echoes produced by fish schools and single fishes from the hydro-acoustic data. To this aim, echograms collected by the echo-sounder with the frequency 418 kHz were also used. The visual comparison of the echograms collected with the two frequencies allowed to make organisms selection easier. During day time this approach permitted to mark as "noisy regions" both the fish schools and areas affected by noise.

During the night fish disperse in the water column, and it was not possible to adopt the same procedure for detecting fish, zooplankton and larvae since single fish are mixed with zooplankton and fish larvae. In this case an automatic selection procedure was adopted; a threshold level for volume backscattering strength (Sv, dB) was set, and signals higher than this level were automatically removed from the processing (Swartzman *et al.*, 1999).

The choice of a threshold level for volume backscattering strength is not simple and it can lead to large errors in the echo-integration analysis. For this reason, all the echograms collected during day time were analyzed for the definition of a maximum value of volume backscattering strength for zooplankton and fish-larvae. This resulted in setting a Sv threshold level at -56 dB and higher signals were automatically excluded from processing.

The next step in both methods was the separation of zooplankton $NASC_Z$ and fish-larvae $NASC_L$ by means of weights ratios. It should be noted that this procedure can lead to big mistakes, as it is based on the assumption that organisms with equal weight have equal backscattering signals. Even though this is generally not true, this hypothesis was made because species composition of zooplankton was not available for the collected biological samples.

As the weights ratio was estimated in all the biological stations located in the sampling grid (12 nm) and NASC values were evaluated along the vessel track (each nautical mile), the weight ratio of the i^{th} station was used to calculate $NASC_Z$ and $NASC_L$ in the EDSUs closest to the station.

In the *first method* outlined in Figure 9, other two steps were necessary to estimate, NASC values belonging to anchovy larvae with swim-bladder, anchovy larvae without swim-bladder and other species larvae (HL). These estimates were based on the ratios between number of specimens. For anchovy larvae with swim bladder (LA+) the relationship between target strength (TS, dB) and standard length (SL, cm) was used (Gontcharov *et al*., 2002)

$$TS = 20 \cdot \log_{10}(SL) - 77.11 \quad \text{(dB)}.$$

For anchovy specimens without swim bladder (LA-) a constant target strength of -88 dB, experimentally estimated (Gontcharov *et al*., 2002), was adopted.

The average SL values of anchovy larvae in each station were used for estimating TS. The backscattering cross-section of larvae specimens (σ_{bs}, m^2) was then calculated by the formula (MacLennan *et al.*, 1991):

$$\sigma_{bs} = 10^{TS/10} \quad (m^2)$$

Surface densities of anchovy larvae ρ_{LA} have been calculated for each ESDU by the following formulas:

$$\rho_{LA+} = n_{LA+} \cdot \frac{NASC_{LA} \cdot \overline{w}_{LA+}}{4 \cdot \pi \cdot \left(n_{LA+} \cdot \overline{\sigma}_{LA+} + n_{LA-} \cdot \overline{\sigma}_{LA-} \right)} \quad (g/nmi^2);$$

$$\rho_{LA-} = n_{LA-} \cdot \frac{NASC_{LA} \cdot \overline{w}_{LA-}}{4 \cdot \pi \cdot \left(n_{LA+} \cdot \overline{\sigma}_{LA+} + n_{LA-} \cdot \overline{\sigma}_{LA-} \right)} \quad (g/nmi^2);$$

$$\rho_{LA} = \rho_{LA+} + \rho_{LA-} \quad (g/nmi^2);$$

where: $\overline{w}_{LA+}$ (g), $\overline{w}_{LA-}$ (g) are the mean weights of LA+ and LA-

$\overline{\sigma}_{LA+}$ (m^2) and $\overline{\sigma}_{LA-}$ (m^2) are the mean backscattering cross-sections of LA+ and LA-

n_{LA+} and n_{LA-} are the numbers of LA+ and LA- specimens.

In each ESDU the anchovy larvae density is obtained by summing the densities of LA+ and LA-.

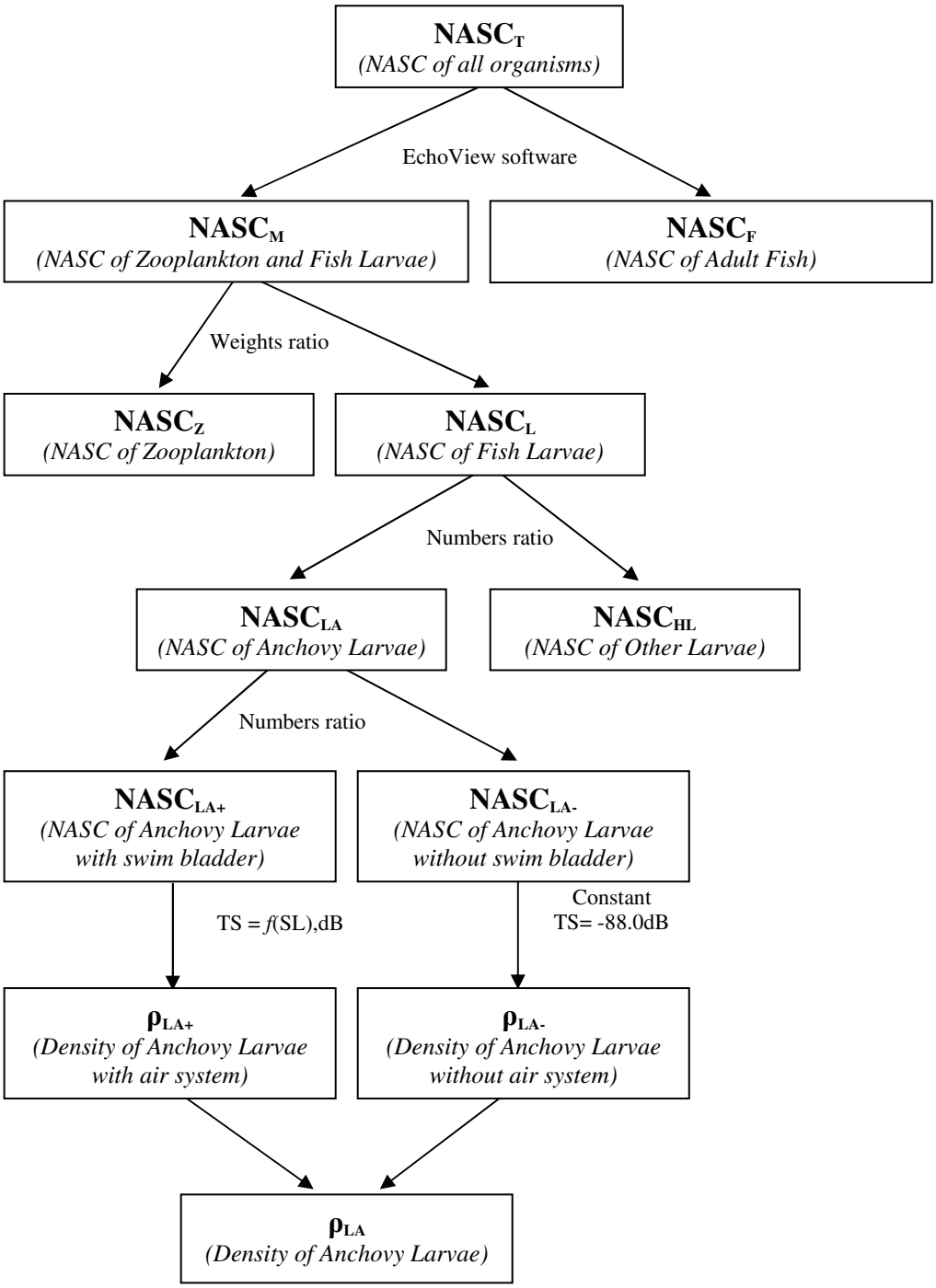

Figure 9. Scheme of the procedure adopted in the First Method to estimate densities of the target species.

The *second method* (Figure 10) considers the TS equation mentioned above for all the larvae (anchovy or other species) with air system ($TS = 20 \cdot \log_{10}(SL) - 77.11$), while for all the larvae without air system the TS was estimated by a mathematical model.

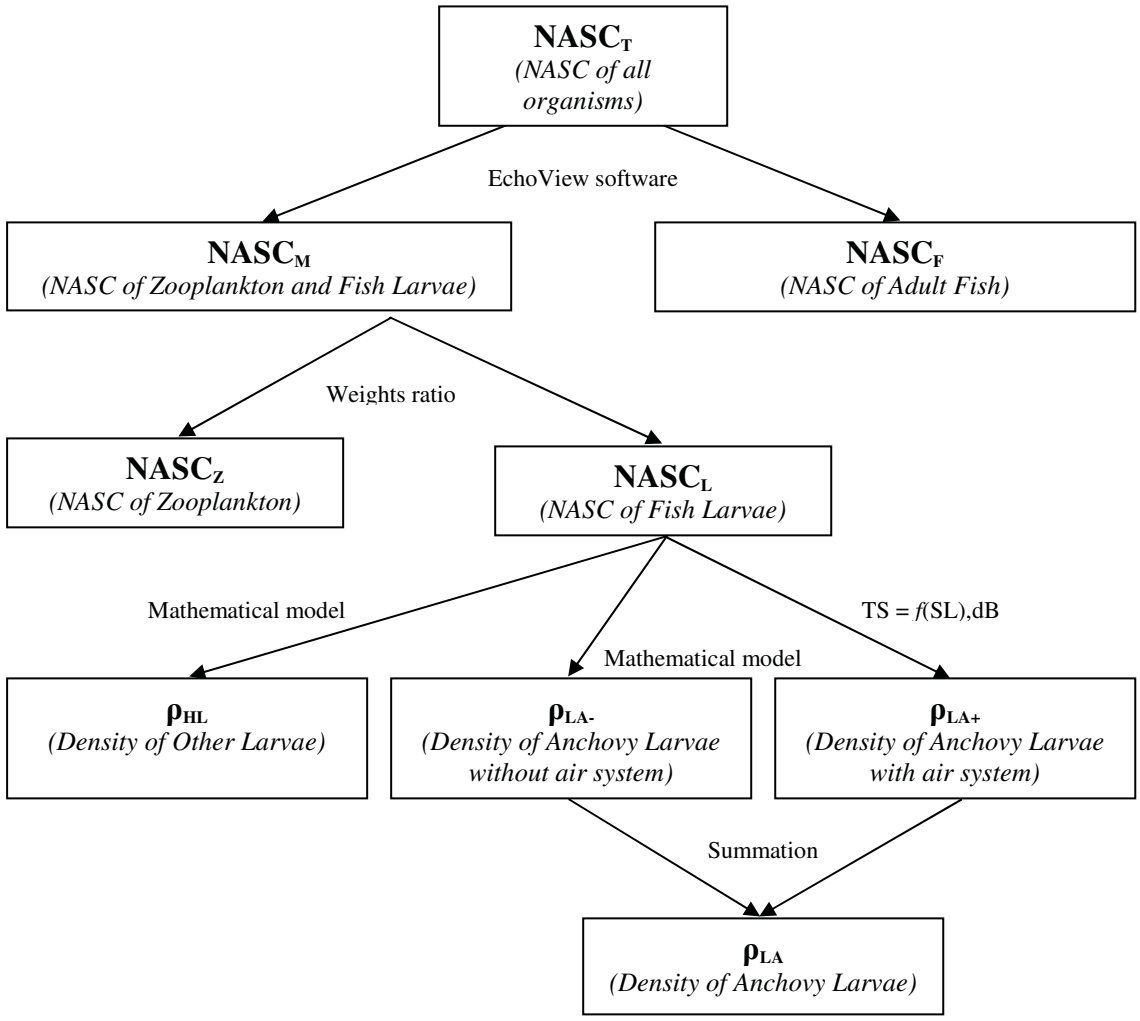

Figure 10. Scheme of the procedure adopted in the Second Method to estimate densities of the target species.

The application of the second method was subordinated to larvae measurements in the ichthyoplankton laboratory.

The σ_{LA+} was estimated with the same procedure of the first method, while the backscattering cross section of anchovy larvae without swim bladder and other species larvae (σ_{LA-} and σ_{HL}) were estimated by the fluid cylinder mathematical model (Gontcharov *et al.*, 2002). According to this model, the backscattering cross-section can be expressed by the formula (Stanton, 1989):

$$\sigma_{bs} = \frac{\frac{1}{4} \cdot L^2 \cdot (k \cdot a)^4 \cdot \alpha^2}{1 + \frac{(\pi \cdot (k \cdot a)^3 \cdot \alpha^2)}{R^2}} \quad (\mathrm{m}^2);$$

$$\alpha = \frac{1 - g \cdot h^2}{2 \cdot g \cdot h^2} + \frac{1 - g}{1 + g};$$

$$R = \frac{g \cdot h - 1}{g \cdot h + 1};$$

where: a (m) is the radius of the equivalent cylindrical volume of the specimen

L (m) is the equivalent cylinder height

g is the ratio between the cylinder density and the surrounding medium density (i.e. density contrast)

h is the ratio between the sound speed inside the cylinder and that one in the surrounding medium (i.e. sound-speed contrast)

k is the wave number obtained from the expression described below

$$k = \frac{2 \cdot \pi \cdot f}{c}$$

where f (Hz) is the wave frequency and c (m/sec) is the sound speed in the medium.

Surface densities of fish larvae were calculated for each integration point by the formulas:

$$\rho_{LA+} = \frac{NASC_L \cdot \sum w_{LA+}}{4 \cdot \pi \cdot (\sum \sigma_{LA+} + \sum \sigma_{LA-} + \sum \sigma_{HL})}, \text{ (g/nmi}^2\text{)};$$

$$\rho_{LA-} = \frac{NASC_L \cdot \sum w_{LA-}}{4 \cdot \pi \cdot (\sum \sigma_{LA+} + \sum \sigma_{LA-} + \sum \sigma_{HL})}, \text{ (g/nmi}^2\text{)};$$

$$\rho_{HL} = \frac{NASC_L \cdot \sum w_{HL}}{4 \cdot \pi \cdot (\sum \sigma_{LA+} + \sum \sigma_{LA-} + \sum \sigma_{HL})}, \text{ (g/nmi}^2\text{)};$$

or:

$$\rho_{LA+} = \frac{NASC_L \cdot n_{LA+}}{4 \cdot \pi \cdot (\sum \sigma_{LA+} + \sum \sigma_{LA-} + \sum \sigma_{HL})}, \text{ (ind/nmi}^2\text{)};$$

$$\rho_{LA-} = \frac{NASC_L \cdot n_{LA-}}{4 \cdot \pi \cdot (\sum \sigma_{LA+} + \sum \sigma_{LA-} + \sum \sigma_{HL})}, \text{ (ind/nmi}^2\text{)};$$

$$\rho_{HL} = \frac{NASC_L \cdot n_{HL}}{4 \cdot \pi \cdot (\sum \sigma_{LA+} + \sum \sigma_{LA-} + \sum \sigma_{HL})}, \text{ (ind/nmi}^2\text{)};$$

$$\rho_{LA} = \rho_{LA+} + \rho_{LA-};$$

where: w_{LA+} (g), w_{LA-} (g), w_{HL} (g) are individual weights of LA+, LA- and HL

σ_{LA+} (m^2), σ_{LA-} (m^2) and σ_{HL} (m^2) are individual backscattering cross sections of LA+, LA- and HL

n_{LA+}, n_{LA-} and n_{HL} are the numbers of LA+, LA- and HL individuals.

The graphic representation of results was carried out by means of the Surfer software package (Golden Software, Inc). For the stations position, the cartographical projection formulas of Mercator equiangular cylindrical projection, with metric coordinates according to the reference ellipsoid of Krasovsky, were used. The "Kriging" geostatistical gridding method was used for estimating fish larvae biomass; the experimental omnidirectional standardized variograms were calculated and fitted, by visual adjustment, to logarithmic model.

3.2.2 Results

The echograms show the typical aggregations recorded in Libyan waters like single fish, fish schools and ichthyoplankton layers or patches.

The anchovy larvae density (ind/m^2) along the survey track is shown in Figure 11, while Figure 12 presents the density (ind/m^2) of other species larvae.

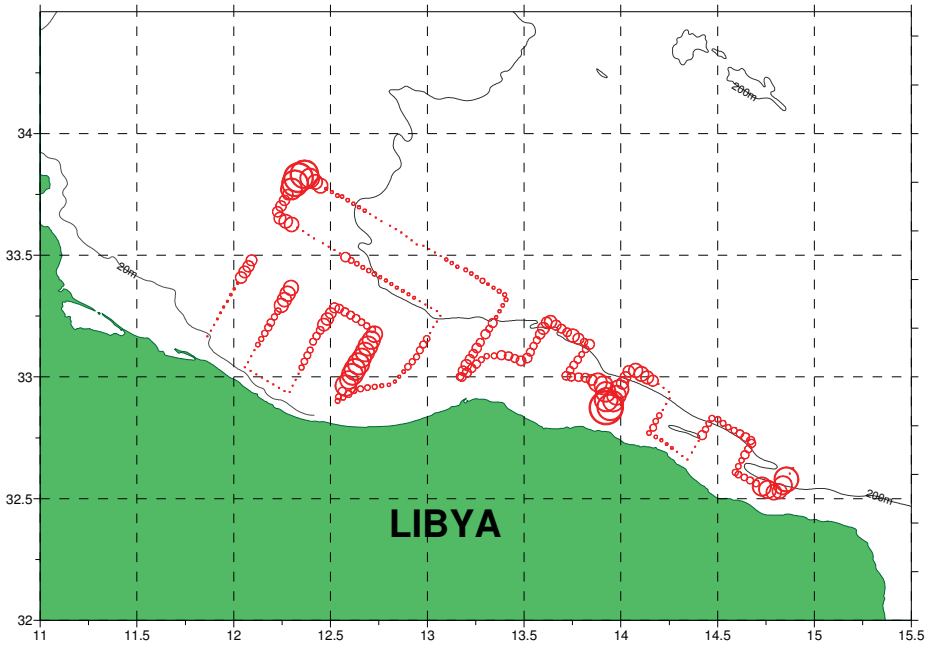

Figure 11. Map of the anchovy larvae density (ind/m^2) distribution.

Both figures show the results of the application of the above described second method. Both figures are in agreement with the biological sampling results described in the section 5.1.2 of the present report.

A comparison between the results obtained for anchovy larvae by the two methods is reported in Table 1. The second method estimates a higher density of anchovy larvae with swim bladder and a lower density of anchovy larvae without air system than the first method. This is mainly due to the low constant TS value associated to all the small organisms without swim

bladder. The mathematical model probably gives a better approximation of the target strength of such larvae.

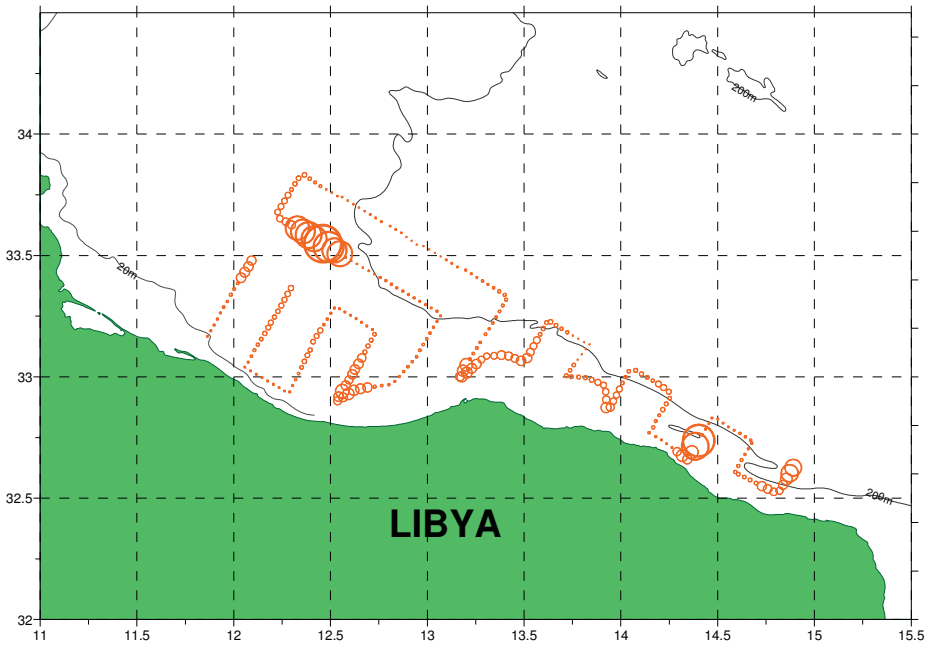

Figure 12. Map of the density (ind/m^2) distribution of other species larvae.

Table 1. Results of the two methods used for anchovy larvae biomass estimation.

ind/nmi^2	FIRST METHOD			SECOND METHOD		
	LA+ density	LA- density	LA density	LA+ density	LA- density	LA density
Mean	**2,145,795**	**6,363,522**	**8,509,317**	**2,339,452**	**5,424,620**	**7,764,072**
Standard Error	152241.5	316292.2	407484.7	187574.2	299498.1	426972.8
Standard Deviation	5079027.0	10552031.4	13594362.2	6257785.7	9991752.6	14244518.7
Maximum	51954907	88219127	113078326	60630167	96786719	131959774
Count	1113	1113	1113	1113	1113	1113
Confidence Level (95.0%)	298712.9	620596.8	799525.5	368039.3	587645.1	837763.1

g/nmi^2	FIRST METHOD			SECOND METHOD		
	LA+ density	LA- density	LA density	LA+ density	LA- density	LA density
Mean	**9632,9**	**9245,2**	**18878,0**	**10897,6**	**4583,9**	**15481,6**
Standard Error	775.4	761.4	1171.6	966.6	211.3	1113.1
Standard Deviation	25869.5	25400.6	39086.1	32248.6	7047.7	37134.3
Maximum	279181.2	294063.8	335109.1	325798.0	65266.6	391064.6
Count	1113	1113	1113	1113	1113	1113
Confidence Level (95.0%)	1521.5	1493.9	2298.8	1896.6	414.5	2184.0

3.2.3 Conclusion

These results have to be considered as a first step towards the implementation of an appropriate method for estimating larvae biomass in the Libyan waters. A further improvement of the method is linked to the opportunity to perform the analysis of species

composition for zooplankton. This will permit to accurately divide the $NASC_M$ of small organisms to each larvae specimen or each zooplanktonic specimen.

4 Oceanography

The main objective of this part of the research activity was to study the water masses circulation in the western Libyan sea area. It is important to single out that in such area no oceanographic data have been collected in the last decade, so the sea water circulation in the study area was studied only by means of mathematical models.

The collected profiles of the oceanographic variables will permit to evaluate the structure of the water column and to recognize water layers of different origins. Moreover, during the survey MedSudMed-06, for the first time, hydrographical data along a transect between the Sicilian and the Libyan coasts were collected. Such section can give an idea of the structure both of the Modified Atlantic Water and the Levantine Intermediate Water along the section.

4.1 Material and methods

A detailed grid of 56 hydrographic profiles covered the region from the very shallow water (23 m) along the coast to about 700 m depth along the continental slope. In all the hydrological stations, continuous vertical profiles of conductivity, temperature, pressure fluorescence and dissolved oxygen were obtained from the surface to the bottom by means of a CTD-rosette system consisting of a CTD SBE 911 plus, and a General Oceanics rosette with 24 Niskin Bottles. The hydrological data were collected every 12 nm, in 56 stations in Libyan waters and in the central part of the Strait of Sicily (see Figure 1). Moreover, CTD data were also acquired in 11 stations in the Italian and Maltese waters.

The probes were calibrated before and after the cruise at the NURC (NATO Undersea Research Centre) in La Spezia, Italy. Simultaneous vertical profiles of horizontal current have been acquired using a Lowered Acoustic Doppler Current Profiler system (LADCP model WH Sentinel of RDI Instruments), in collaboration with scientists from the ISMAR-CNR of La Spezia (Italy). All data have been processed using SBE (SeaBird Electronics) standard software for the hydrographic data, while currents are computed applying the LDEO (Lamont-Doherty Earth Observatory, Columbia University) processing software, developed by Visbeck (2002). The Ocean Data View software package (http://www.awi-bremerhaven.de/GEO/ODV, 2005) was used to plot profiles, sections and surfaces of the acquired oceanographic data.

4.2 Results

Temperature and salinity profiles of the 56 hydrological stations on the Libyan shelf are shown (as scatter-plots) in Figure 13. The temperature profiles single out a well developed thermocline at a mean depth of about 27 m, and a progressive decrease of temperature from about 28 °C at the surface to 13.6 °C near the bottom. It is worth noting two different decreasing trends of temperature for the stations deeper than 250 m; in particular, the deeper stations, located in the most external transects parallel to the coast, have a lower temperature gradient in the depth layer 150-250 (Figure 14).

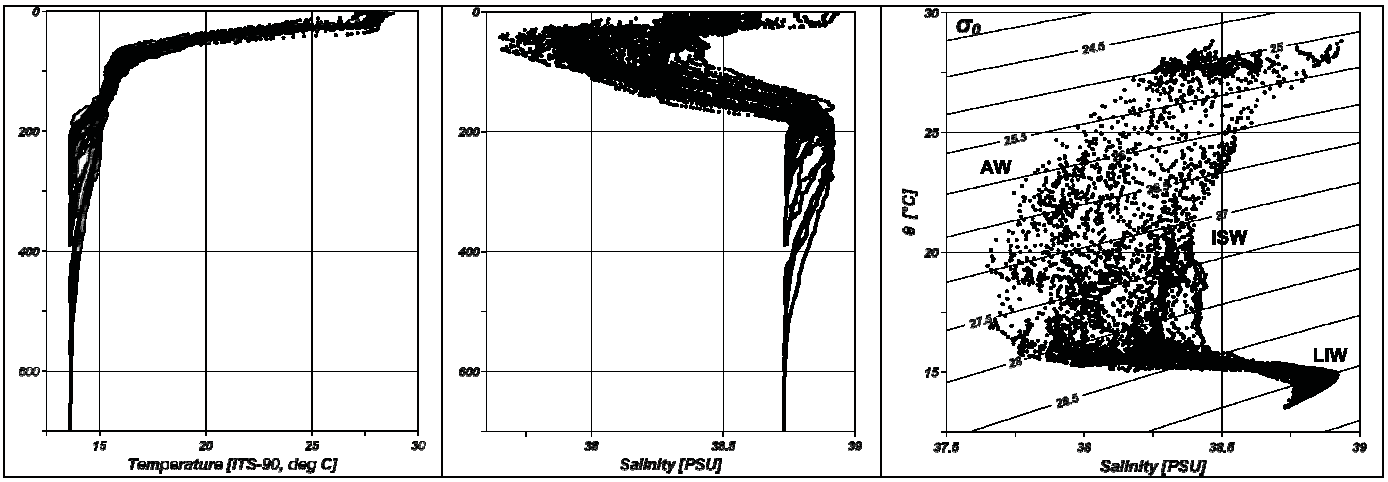

Figure 13. Temperature and salinity vertical profiles of the 56 hydrological stations on the Libyan shelf. On the right side the acquired 56 profiles are shown on the θ/S diagram.

The salinity profiles evidence the AW (Atlantic Water) signature with a minimum (Smin) at about 75 m. The successive increase reaches its maximum (Smax) at about 175 m (Levantine Intermediate Water, LIW core). Going deeper, both temperature and salinity appear almost constant near the bottom, evidencing a homogeneous bottom layer of about 50-70 m thickness.

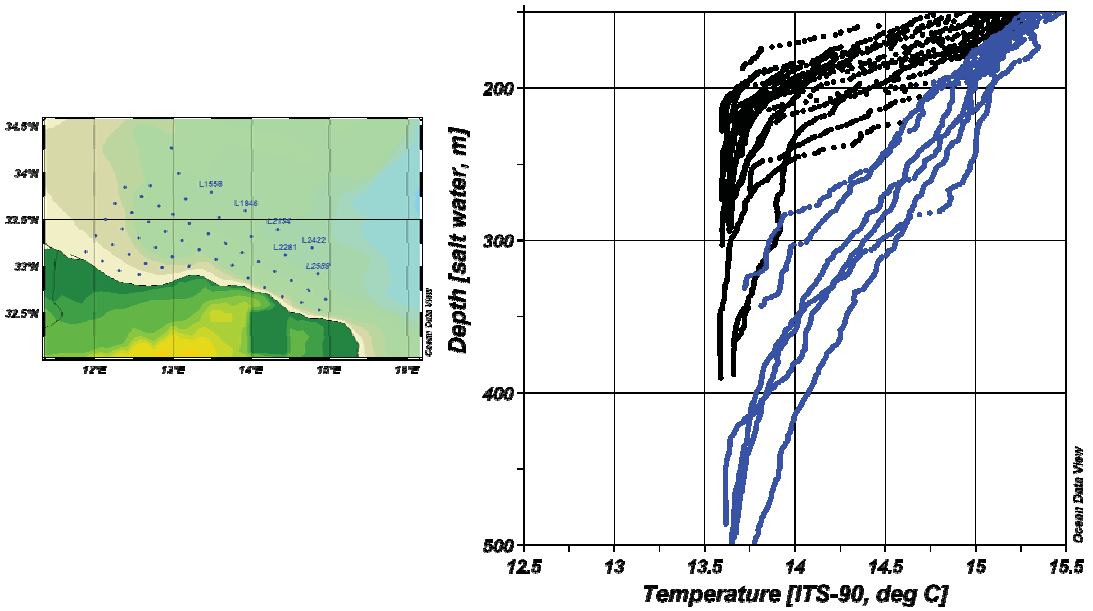

Figure 14. Temperature profiles of the 56 hydrological stations on the Libyan shelf in the depth layer 150-500 m. Blue profiles refer to the stations less influenced by AW.

The horizontal map of the salinity minimum (Smin) in Figure 15a evidences a westward intrusion of fresher water along the coast, with the core at about 50-70 m depth. Its presence is well defined on the western side, while it becomes very thin moving eastward. The Smin distribution evidences several fragmented structures, suggesting the interaction between two different water masses: the AW, moving eastward, and the Ionian Surface Water (ISW), which moves in the opposite direction.

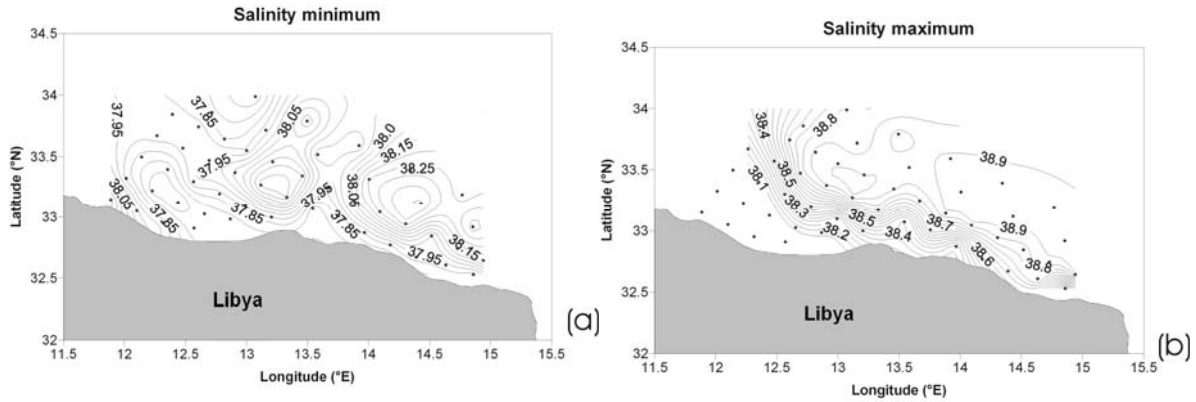

Figure 15. Horizontal distribution of (a) minimum of salinity (S_{min}) and (b) maximum of salinity (S_{max}).

In Figure 16 the temperature and salinity profiles of the stations L1270 and L2134 show an example of the different structure of the water column. In particular, the AW is evident in the upper water layer of the station L1270, while the ISW corresponds to the upper layer in the station L2134.

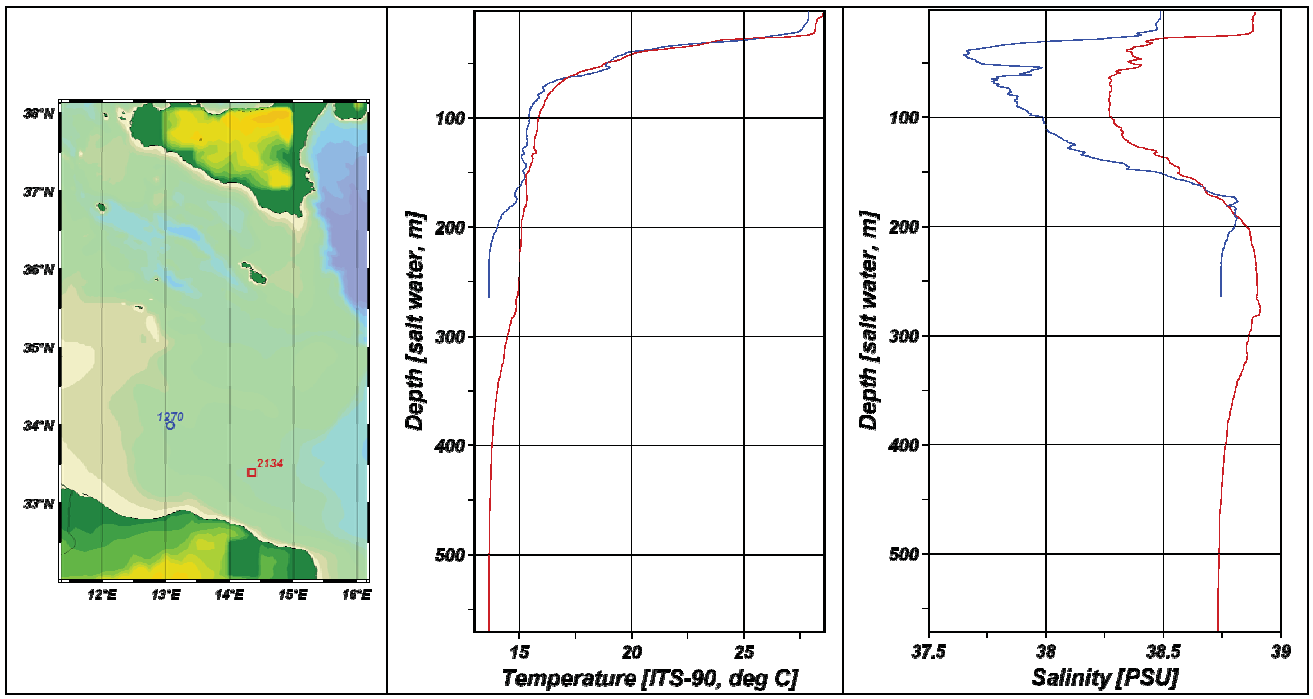

Figure 16. Structure of the sea water masses in the stations L1270 and L2134.

The salinity maximum (Smax), the signature of the LIW core, shows values ranging from 38.92 to 38.71 (Figure 13 and Figure 15b). The Smax is found below 200 m in the deep region, while along the continental shelf it is positioned at about 160-180 m. Its distribution appears more regular than that of Smin, even if some small structures may be observed, probably due to topographic effects. Salinity clearly decreases moving from east to west, confirming a prevalent westward spreading of the LIW.

The interpretation of water masses movements has been conducted using both the current measurements of the LADCP and the estimated geostrophic currents. In Figure 17 to Figure 20 the geostrophic currents for depths 25, 75, 100 and 150 m are shown together with LADCP measurements, averaged in a 40-50 m thickness layer centred at the same depths.

The currents pattern at 25 m depth (Figure 17) is quite complex since it is the result of interaction between AW and saltier ISW. In the western side of the study area it is evident the slow eastward movement of AW; in the central part and in the easternmost area the AW flows along the Libyan coasts in a narrower sea area.

In the eastern side of the area is present a cyclonic structure generated by the opposite movement of AW and ISW. The geostrophic velocity field at 25 m depth (right side of Figure 17) is in agreement with LADCP measurements in the eastern and in the western parts of the surveyed area, while there is not a good matching in the central part where some fragmented structures are present.

The currents pattern at 75 m depth is very similar to the one at 25 m. The cyclonic vortex in the eastern area and the complex structures in the central part are evident, while the AW tends to occupy a thinner coastal area flowing eastward. At this depth there is a better agreement between geostrophic velocities and LADCP measurements (Figure 18).

At 100 m depth the current movement in more coastal waters of the western area assumes a westward direction favouring the formation of a small anticyclonic circulation. In the central and western parts of the area the current flows westward meandering. There is a good agreement between LADCP measurements and the estimated geostrophic currents (Figure 19).

The circulation pattern at 150 m depth reveals a slow anticyclonic circulation in almost all the area (Figure 20). In the western part, in particular, the anticyclonic vortex is more evident than at 100 m depth (Figure 19).

Description of the cold vein

The Libyan coast is smooth and the bottom topography along the continental margin is characterized by a roughly flat region. The continental platform shows a wide extension in the Gulf of Syrta (approximately 80 km), slightly reduces moving westward, but significantly expands towards Tunisia. Along the continental margin several canyons can be observed, with the most pronounced one positioned in front of Tripoli. These topographic characteristics are important because they intensely interact with the coastal current.

An interesting peculiarity of this region is the vertical structure of temperature along the continental slope, which shows a steep decrease at 200-300 m depth, immediately below the LIW (Figure 13 and Figure 21). This water is also characterized by high salinities generally above 38.73. High salinity and low temperature result in density greater than 29.17 along the continental slope. Outside the continental margin the same temperature and density are found significantly deeper (600-700 m) (Figure 13 and Figure 21b). All these characteristics suggest the presence of a dense vein, flowing westward and trapped along the continental slope. This water mass is also characterised by a higher oxygen content than the surrounding LIW.

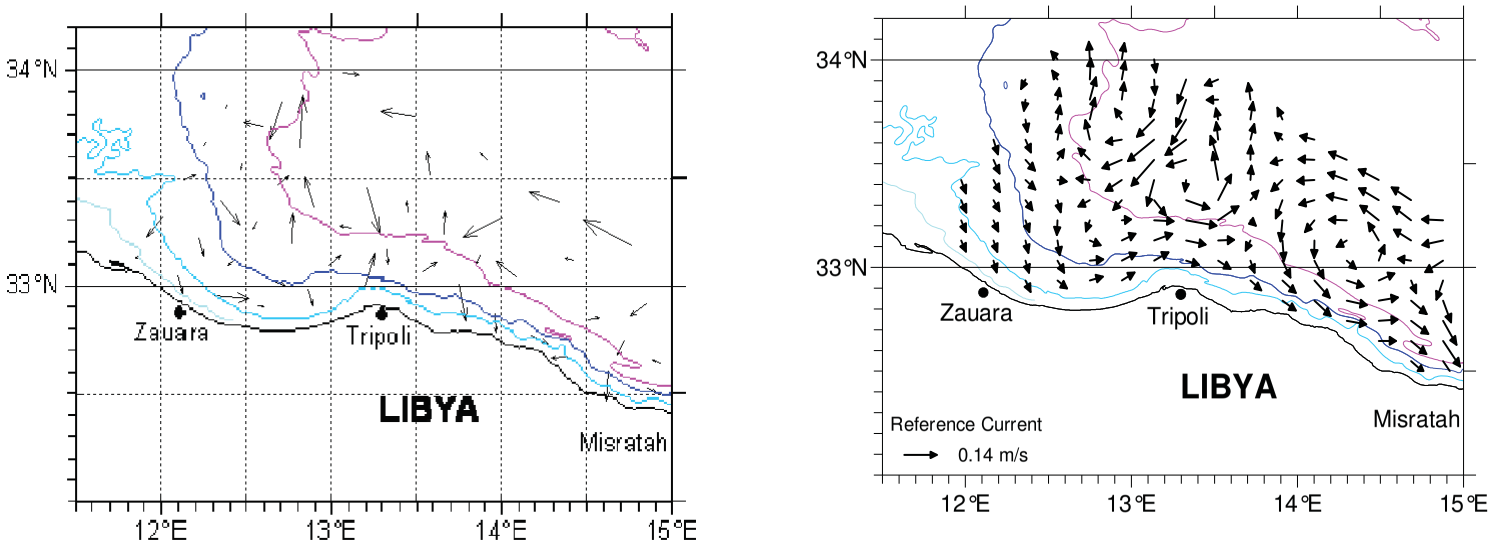

Figure 17. Mean values of current speed evaluated by LADCP in the layer 0 – 40 m (on the left) and Geostrophic currents at 25 m (on the right).

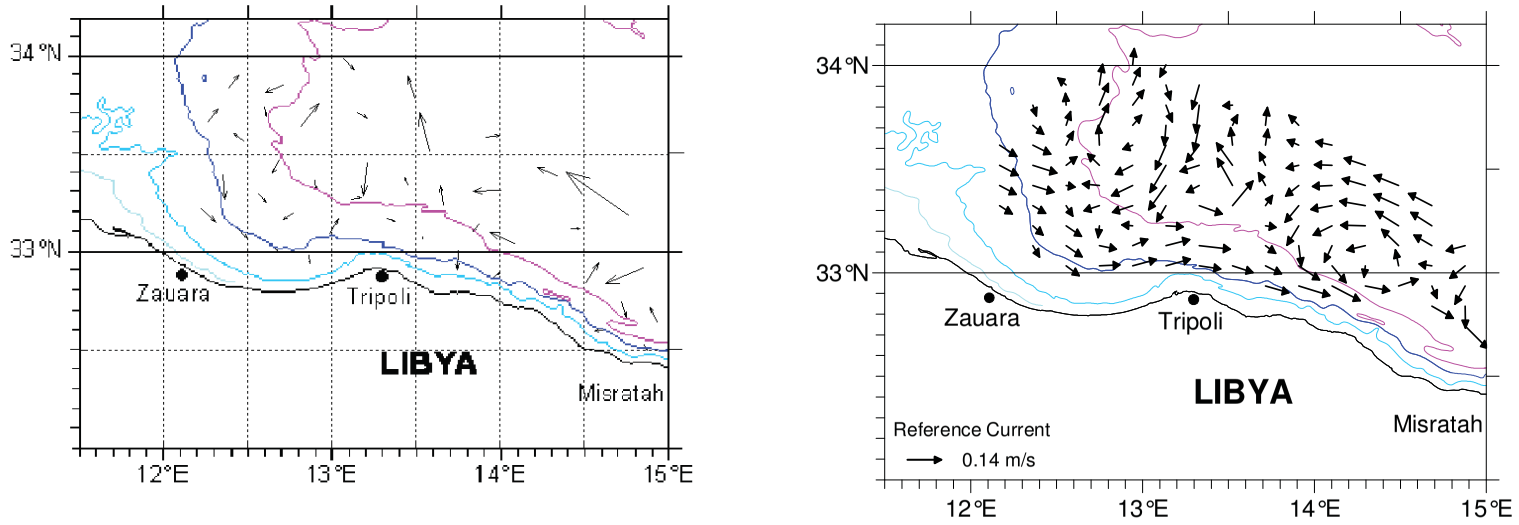

Figure 18. Mean values of current speed evaluated by LADCP in the layer 50 – 90 m (on the left) and Geostrophic currents at 75 m (on the right)

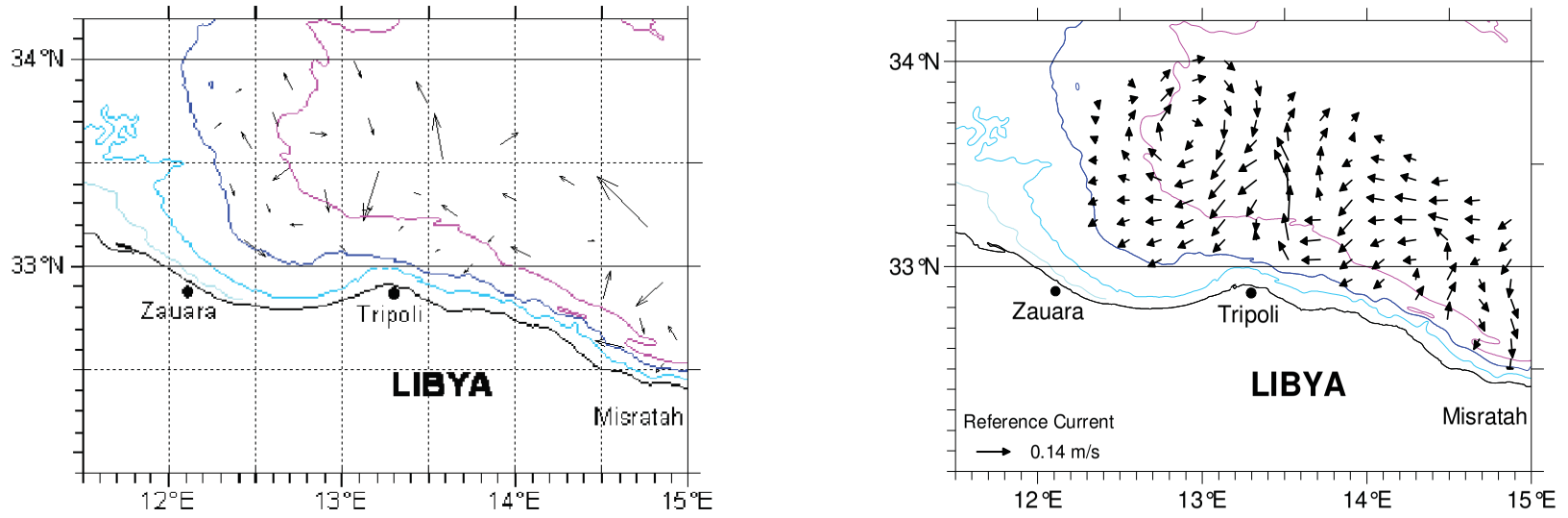

Figure 19. Mean values of current speed evaluated by LADCP in the layer 90 – 120 m (on the left) and Geostrophic currents at 100 m (on the right).

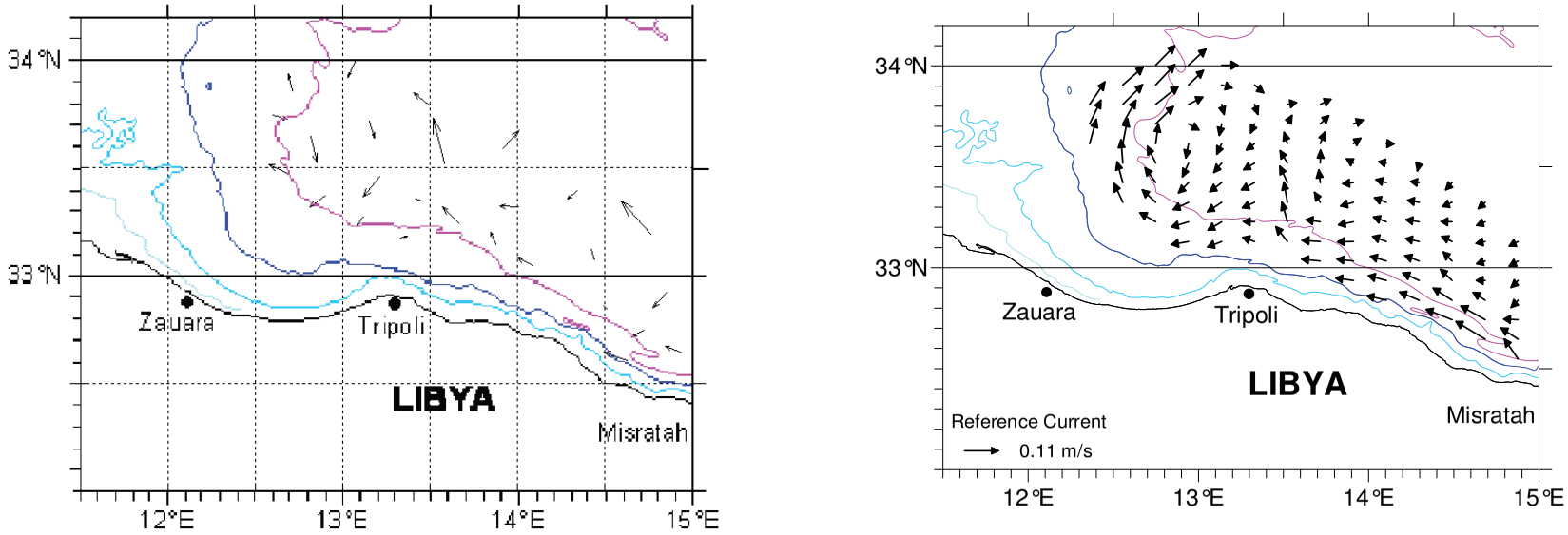

Figure 20. Mean values of current speed evaluated by LADCP in the layer 130 – 170 m (on the left) and Geostrophic currents at 150 m (on the right).

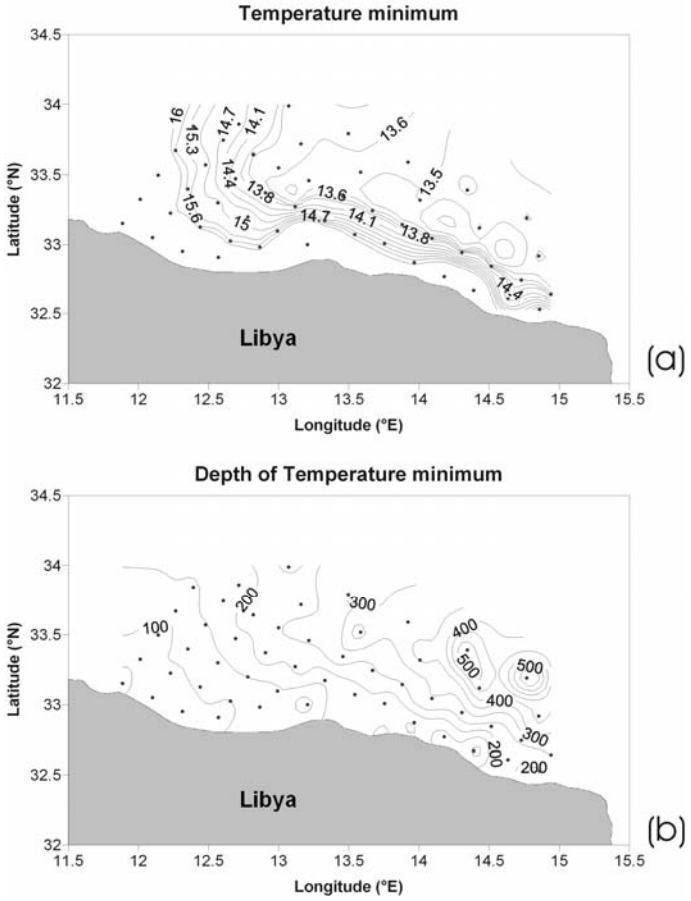

Figure 21. **Horizontal distribution of (a) minimum of potential temperature (θ_{min}) and (b) depth of θ_{min}.**

The analysis of the hydrographic and dynamic characteristics of each profile allowed selecting those stations which are in the path of the vein and tracking its trajectory (Figure 22). After a roughly straight path, a sudden turn is observed in correspondence with 13°E (station L1564b), where a marked canyon along the continental margin is evident, deepening along a west-east axis. The vein cannot spread further westward and produces a cascade along the canyon, due to its high density. A new equilibrium is found at about 600-700 m depth. Unfortunately, the lack of hydrographic profiles in the deeper region does not permit to follow the sinking of the vein further.

With the available data it was possible to describe the evolution of the vein characteristics along approximately 195 nm. Assuming the 29.16 isopycnal as the upper boundary of the vein, its thickness is 50-70 m from the easternmost station above the shelf, until its cascading along the canyon. A detailed analysis of the evolution of its hydrographic characteristics evidences two phases. Firstly the vein flows along the flat region and a weak increase of temperature and salinity is observed, due to the mixing with the surrounding LIW.

The thickness of the vein is stable at approximately 50-70 m. In the second phase, this stability is weakened when the vein meets the topographic discontinuity, where it is not able to maintain its depth and begins to sink. Remarkable modifications, due to mixing and entrainment of the resident water, appear when the vein reaches depths below 400 m. Temperature and salinity decrease, while the vein thickness increases significantly up to 200 m at 700 m depth (station L2422).

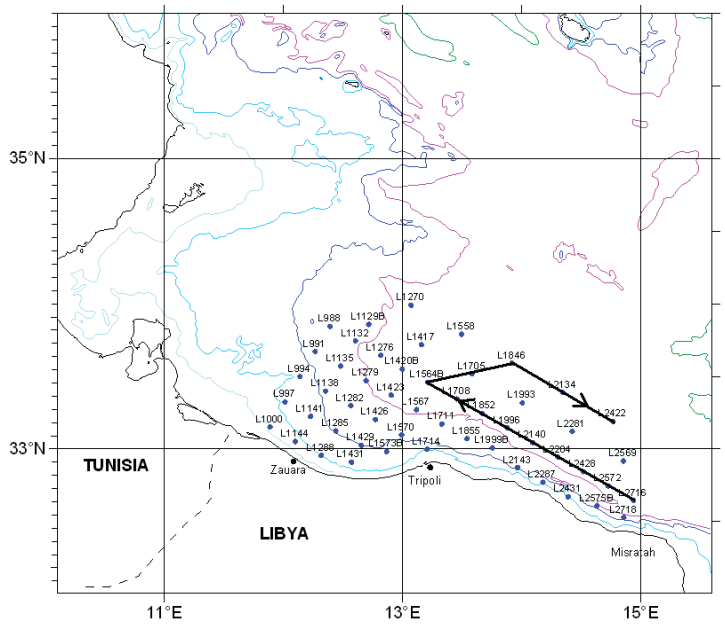

Figure 22. **The investigated region, with the position of the CTD and LADCP stations. The thick line indicates the main trajectory of the vein.**

The analysis of the structure of the horizontal velocity along the transects between the stations L988 and L2716 (Figure 23) highlights the presence of a jet shape in correspondence with the bottom layer, with current speeds of about 6-8 cm/s. This jet is westward in stations L2716, L2572, L2140, L1996, L1852, L1708 and L1564, that is before the vein reaches the canyon north of Tripoli, while its direction is opposite in station L1705 (Figure 24), where the vein begins to sink deeper.

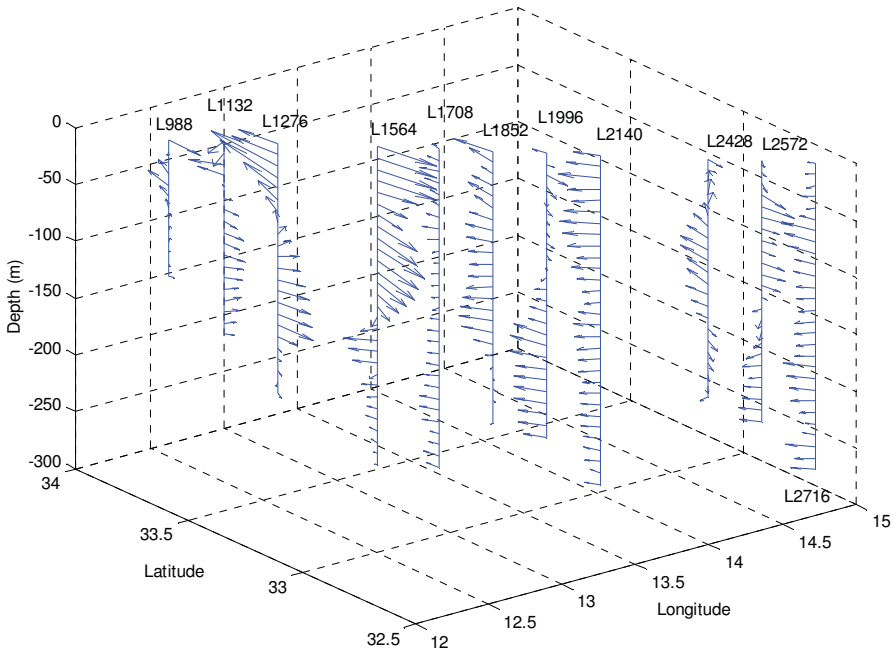

Figure 23. **Current speed profiles evaluated by LADCP along the transects between the stations L988 and L2716.**

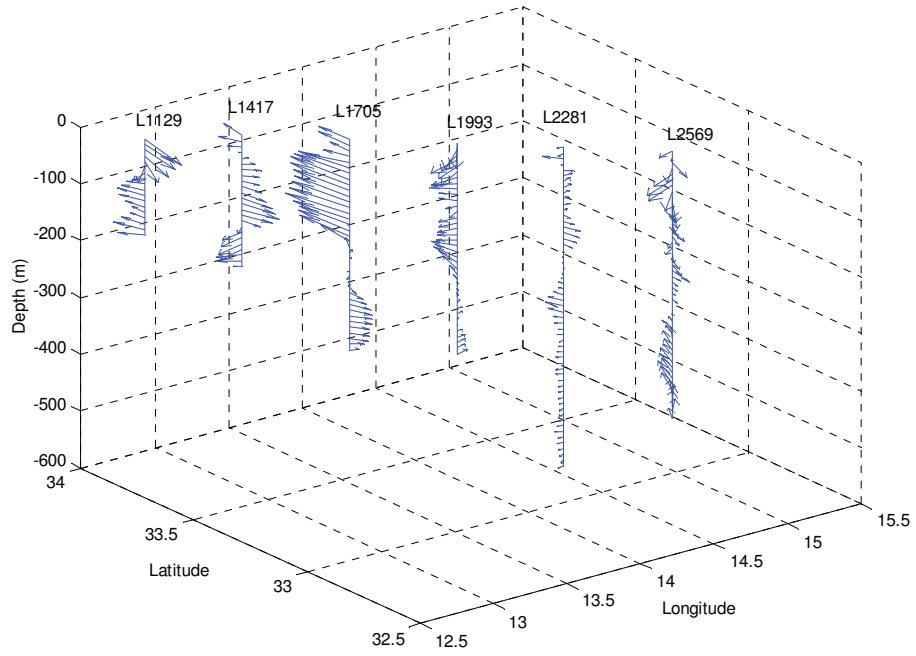

Figure 24. **Current speed profiles evaluated by LADCP along the transects between the stations L1129 and L2569.**

The current velocities in the station L1846 (Figure 25) evidence a clear pattern in the depth layer between 210 and 360 m with speeds of about 5-8 cm/s. In the stations L2134 and L2422 the vein moves in deeper layer with lower current speeds.

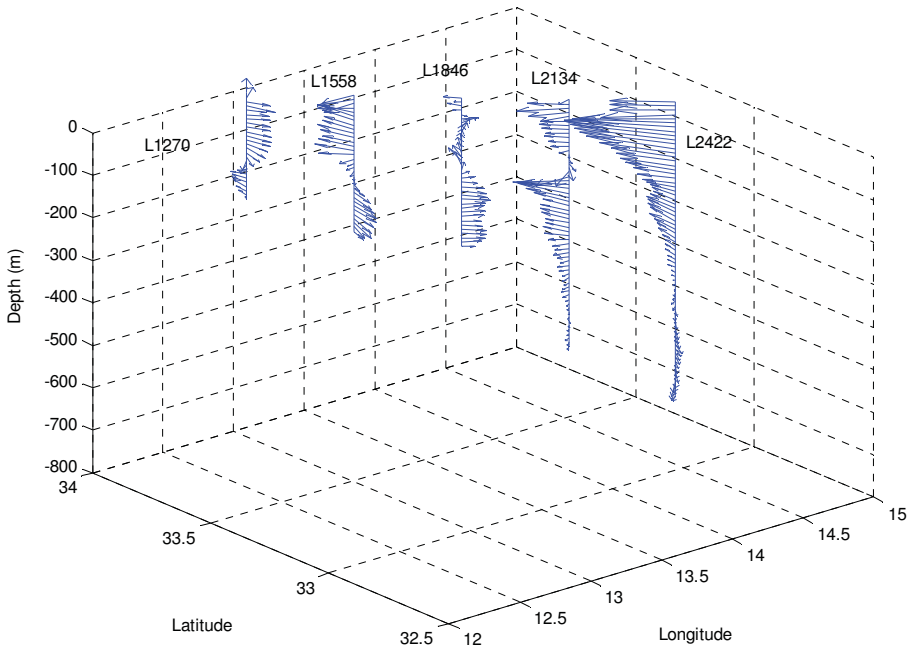

Figure 25. **Current speed profiles evaluated by LADCP in an external transect.**

The transect between the Sicilian and the Libyan coasts

In Figure 26temperature, oxygen, density and salinity fields along the transect are shown.

The salinity section highlights the signature of the AW in the upper layer (about 200 m thick). It is worth noting that the core of the Modified Atlantic Water (MAW), characterized by salinity values less than 37.8 PSU, is located in the northernmost half of the transect, close to Malta and the Sicilian coast. The stations located on the Libyan shelf reveal, as mentioned above, the AW signature at about 75 m. The core of the LIW (maximum of salinity) is positioned at about 240 m depth and is evident only in the central part of the transect, south of Malta.

The temperature field singles out a clear stratification, with higher values in the southern side of the transect. This field shows also the effects of the coastal upwelling, induced by the MAW circulation, along the southern Sicilian coast. The structure of the density field (sigma-theta) is similar to the temperature one, while the oxygen assumes higher values in the AW layer.

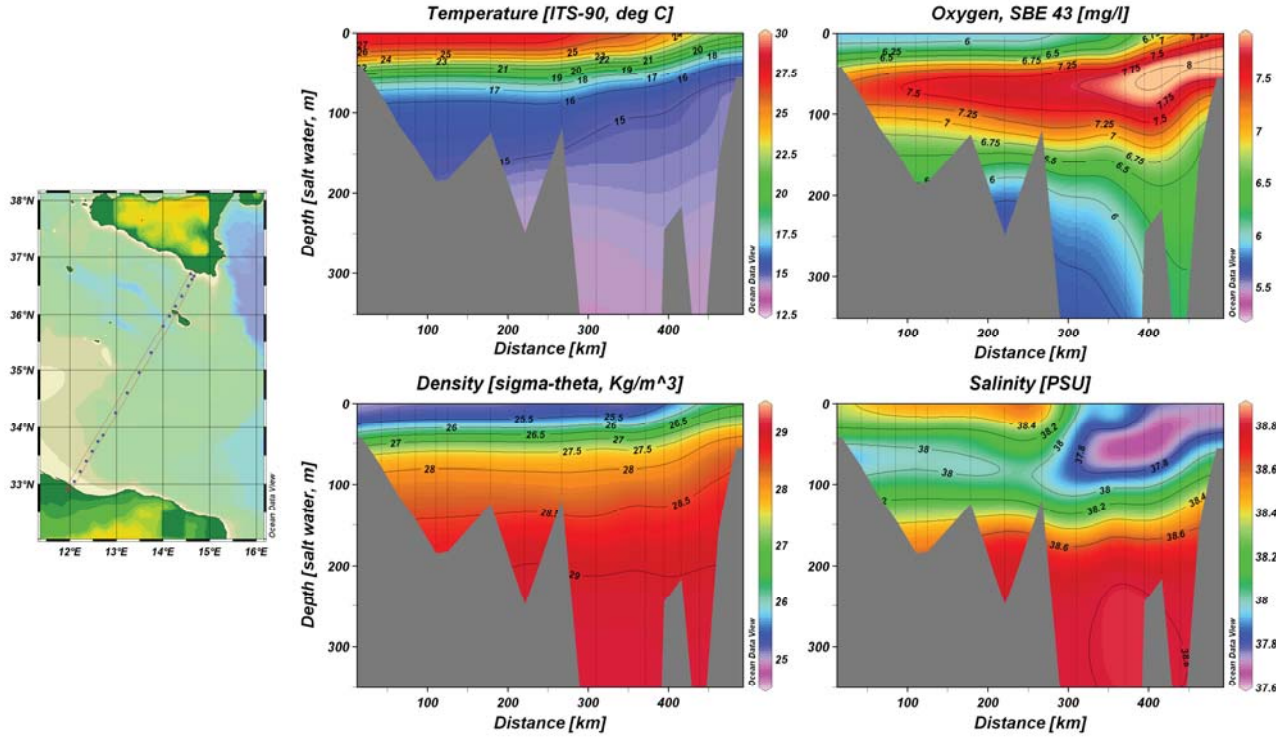

Figure 26. Temperature, oxygen, density and salinity fields along a north-south transect connecting the Sicilian and the Libyan coasts.

4.3 Discussion

The thermohaline characteristics and the water mass circulation along the Libyan coast are poorly known. The little information available provides only a rough description of the hydrographic conditions of the region. Some vertical sections outside the continental margin (Guibout, 1987) suggest that the region has a marginal role in the east-west exchanges, with a small amount of Atlantic Water (AW) and a scarce presence of salty intermediate water. In

the deep layer, close to the bottom, a colder and denser signature can be observed during winter and summer.

The classical Mediterranean circulation schemes (Wüst, 1961; Ovchinnikov, 1966; Lacombe et al., 1981) agree in indicating a prevalent anticyclonic circulation, both in the surface and deep layers. From those schemes no information can be deduced about the surface path of the AW along the African coast, which generally moves from west to east, as suggested by numerical simulations (Béranger et al., 2005). The results of these simulations are in line with classical features, showing an anticyclonic circulation far from the coast, both for the surface and the sub-surface layers.

For the first time a hydrographic survey has been carried out along the western Libyan shelf in summer 2006. It allowed getting evidences on the movement of typical Mediterranean waters (AW, ISW and LIW) shifting in opposite directions along the coast.

In addition to confirming the presence of these well known water masses, the data collected during the survey allowed describing a cold and dense vein flowing along the Libyan margin for the very first time. This vein that has never been detected or foreseen before, flows along the continental slope at about 250-300 m depth and the investigated region corresponds to its final path before it cascades. Its dynamic is generally slow (the speed does not exceed 10 cm/s) with a weak entrainment, especially when the vein flows above the almost constant depth. The entrainment becomes significant when the vein is forced to sink at higher depths due to a topographic discontinuity and its thickness increases from 50 to 200 m. The bottom stress has a prevailing effect, as suggested by the current profile which shows reduced velocities near the bottom and the well mixed vein interior.

The vein seems to have some relevance in the Ionian basin. From available hydrographic data a mean vein width of 20 km can be assumed in the flat region, with a mean thickness of 70 m. Considering an average velocity of 7 cm/s, its transport can be estimated to 0.1 Sv. Even if this value is not that high, the integrated effect is not negligible. Historical data (Gibout, 1987) clearly evidence the presence of cold and dense water in the deep basin (about 1000 m depth) in front of Tripoli. The signature in the historical data suggests that the vein observed during summer 2006 is not episodic and that its buoyancy equilibrium in the Ionian basin can be estimated at about 1500 m depth, which corresponds to the transitional Eastern Mediterranean Deep Water layer (EMDW). For these reasons this vein may have a role in determining the characteristics of the layer below the LIW. From the available data it is not possible to infer the duration of the journey of the vein before reaching the western coast of Libya, but its low oxygen content suggests a quite long time, since this water was in contact with the surface. We also have to consider a slow erosion of the vein, due to the close contact with the surrounding LIW. Furthermore several smaller valleys along the Libyan continental slope are probably responsible for additional vein cascades along the continental slope.

For what concerns its origin, this vein was certainly produced at the surface along the African coast as suggested by its oxygen content, which is low but even higher than that of the surrounding water. It moves westward, probably driven by the large scale circulation, which is anticyclonic in this region. If we suppose a wintertime production (i.e. February) and a constant velocity of 7 cm/s, we can estimate a horizontal spreading of a magnitude of 1000 km, which corresponds roughly to the area off the frontier between Libya and Egypt.

More detailed and extended investigations are necessary in order to better define the importance of the dense vein, its interannual characteristics, its origin and the length of its spreading path.

5 Sediments

5.1 Material and methods

Sediments samples were collected with a box corer that keeps the vertical stratification of the sediments. Samples were collected every 12 nm in the coastal area of Libyan waters in a total of 41 stations. Part of the collected sediments were conserved in PVC tubes in order to maintain the vertical stratification of the sediments, the other part was put in plastic bags to study granulometry and infauna (Figure 27). All sediments were frozen.

Figure 27. Different steps of the sampling with the box corer: PVC tubes and plastic bags

Moreover, prior to each station, a seismic analysis was performed with a Sub-bottom Profiler 3.5 kHz (Chirp) that gives information on the composition of the 1st layer of sediments and on the bottom morphology (Figure 28). Both types of samples allow a geochemical characterization of the most recent sediments (150-200 years), in view of describing the spatio-temporal variation of primary bio-productivity.

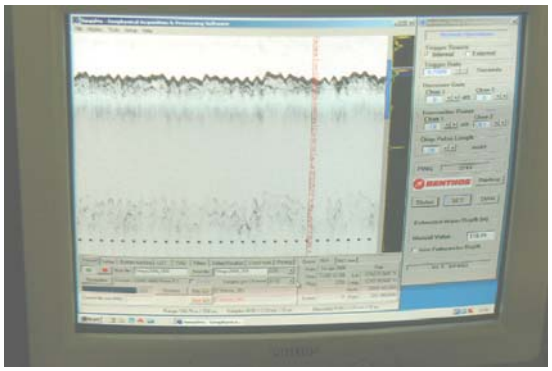

Figure 28. **Example of Chirp display giving an idea on the hardness of the bottom.**

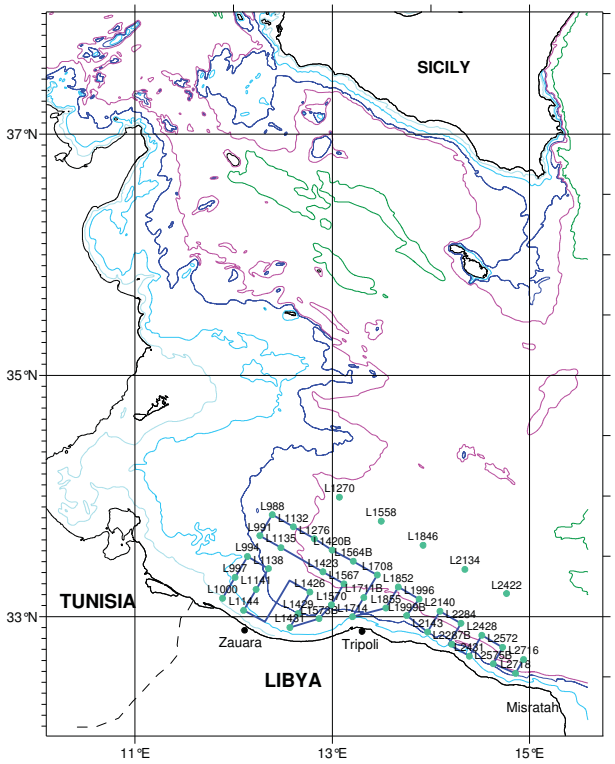

Figure 29. **Position of stations where samples were collected with the Box Corer.**

The steps of the method used to process the samples are listed below:

a. Sediments classification

1- Prior to analysis, the frozen samples were left to thaw at room temperature.
2- A 100g subsample of sediment from each station was used for analysis.
3- The subsample was washed in freshwater in a large two litre beaker several times and finally in distilled water, to remove salt and debris of plants and animals. The sediment was left to settle on the bottom, then the clear water was decanted and the sediment was placed in a wide glass Petri-dish and left to dry in an oven at 100-105°C for 24hrs. The Petri-dish was then taken out to cool.
4- 50g of oven dried sediment was weighed, and then placed on top of a nest of sieves secured on a mechanical sieve shaker (Octagon 200 Test Sieve Shaker) and agitated

mechanically for 15 minutes. The test sieves used had mesh sizes 2.0, 1.0, 0.5, 0.250, 0.125, and 0.063 mm.

5- The sediment was removed from the sieves and any sediment stuck in the mesh was removed by mean of a soft camel-hair brush and added to the previous portion.
6- Each fraction was then weighed to the nearest 0.01g and was expressed as percent dry weight of the initial sample.
7- Cumulative percentages were plotted on probability paper.
8- Phi(ø) values of specific percentiles (16, 50, and 84%) were read from the graphs and were substituted in equation to obtain Graphic mean (M_z) which gives the specific classification of sediment.

Measure of average size (Graphic mean, Mz): $M_z = \frac{\phi 16 + \phi 50 + \phi 84}{3}$

b. Sediments organic matter

For roughly measuring sediment organic matter; 10g of oven dried sediment from each station was placed into a pre-weighted glazed porcelain crucible and was placed into a muffle furnace for ashing. The furnace was set at 600°C and was maintained at this temperature for one hour. After then the crucible was taken out of the furnace and covered with pre-weight aluminium foil and let cool, then reweighed (This was the ash weight).

The organic content (as percentage of dry wt) = 100 x (dry wt – ash wt / dry wt)

5.2 Results

Distribution maps of the different fractions of the sediments are shown below (Figure 30 to Figure 34).

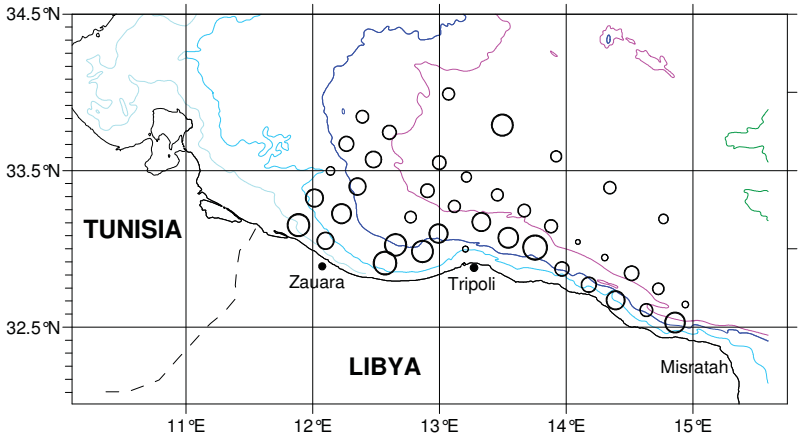

Figure 30. Average size of sediments collected (Graphic Mean, Mz).

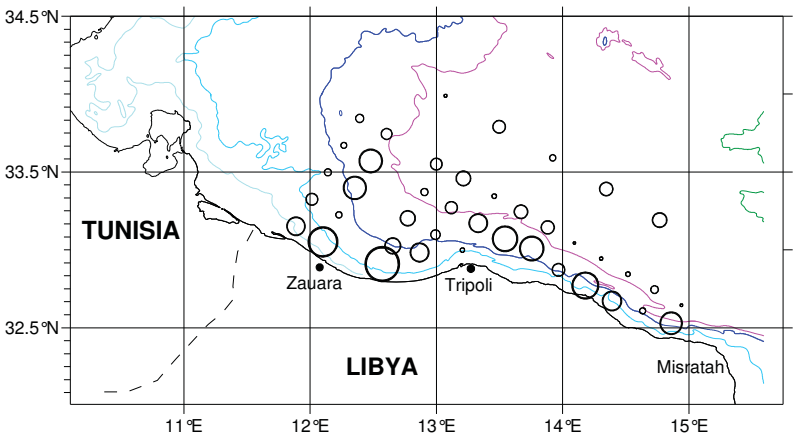

Figure 31. Percentage of organic matter in the sediments collected.

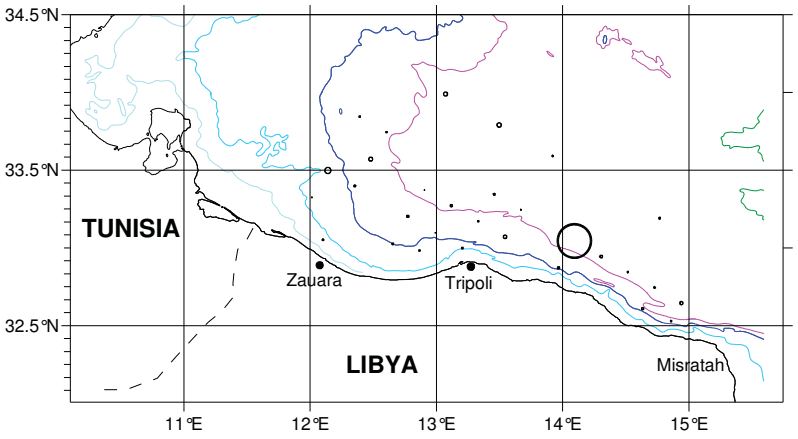

Figure 32. Percentage of gravel in the sediments collected.

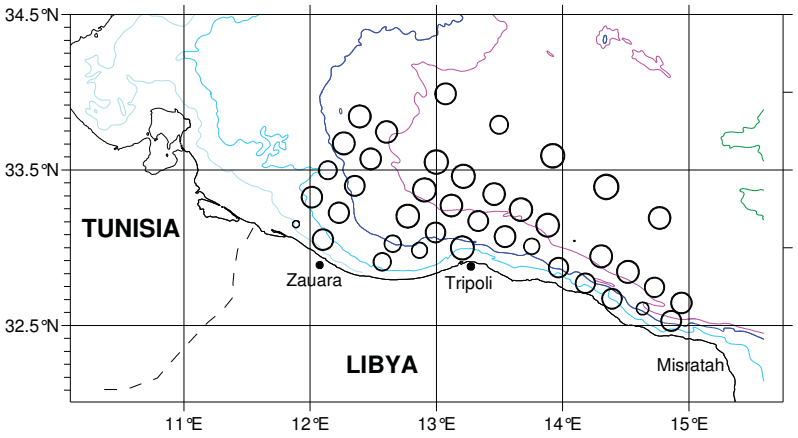

Figure 33. Percentage of sand in the sediments collected.

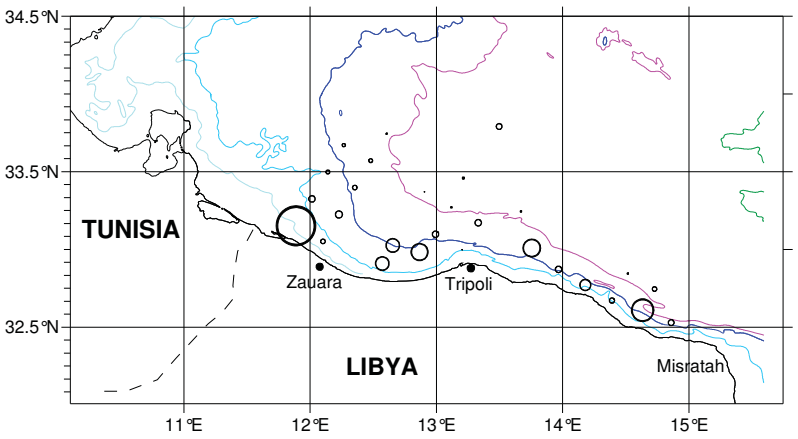

Figure 34. Percentage of mud in the sediments collected

6 Phytoplankton

Phytoplankton is constituted by minute organisms but it is a key component of the oceanic ecosystem. It plays a key role in global biogeochemical cycles, particularly in the carbon-carbonate cycle (Honjo, 1976; Westbroek, 1991; Westbroek et al., 1994), but also in the sulphur cycle since it produces dimethylsulphoniopropionate (DMSP), the precursor of dimethyl sulphide (DMS) (Keller et al., 1989; Malin and Kirst, 1997) which may influence climate through stimulating cloud formation and influencing the Earth's radiative balance (Charlson et al., 1987; Simó and Pedrós-Alió, 1999). Some algae are known to produce stable lipid compounds which can be used as a tool to evaluate paleoclimatic changes (Volkmen et al., 1980; Brassell et al., 1986). These properties, together with the fact that the ubiquitous species *Emiliania huxleyi* is a recognized bloom forming alga (Holligan et al., 1993), confirm that the phytoplankton have an important role as active biogeochemical and climatic agents.

The quantitative analysis focuses on coccolithophore species, hence supplementing previous work carried out at MBRC on diatoms, silicoflagellates and dinoflagellates (Tufail, 1981). Coccolithophyceae should be identified at level of genera and species. The expected output is an atlas to document morphology, taxonomy and diversity of all phytoplankton in the Libyan westernmost coast. The atlas could be inspired by the publication dealing with NW Spain (Cros and Fortuño, 2002). Assessment of abundance (by species and total abundance) and comparison with abundance of eggs and larvae and, possibly, nutrients.

6.1 Material and methods

Samples of waters were collected with Niskin bottles in selected stations for the analysis of phytoplankton, in particular calcareous phytoplankton (Coccolitophyceae). Stations were chosen along transects perpendicular to the coast, the sampling design was then adapted according to the time available, forbidden areas etc. About 500 ml of sea water were filtered, using a vacuum pump, onto polycarbonate Nucleopore filters of 0.2 µm pore size and 47 mm diameter. The filters were dried in an oven for 3h and stored in hermetically closed boxes until preparation for the Scanning Electron Microscope (SEM). To investigate the total thickness of the photic zone we have selected these depth intervals: 0, 25, 50, 100, 150 and 200 metres. A total of 70 samples were collected in 15 stations (Figure 35).

A part of the filter was placed on a SEM stub and coated with a film (about 150 Å thick) of gold-palladium to avoid electric charges; the sputter coater used was a Balzers. The examination and microphotography of the specimens were conducted in a Philips XL30 Scanning Electron Microscope. The filters were then analyzed under electron scanning microscope with the objective of carrying out: qualitative analysis for the identification of species, and quantitative analysis with the enumeration of individuals for each species.

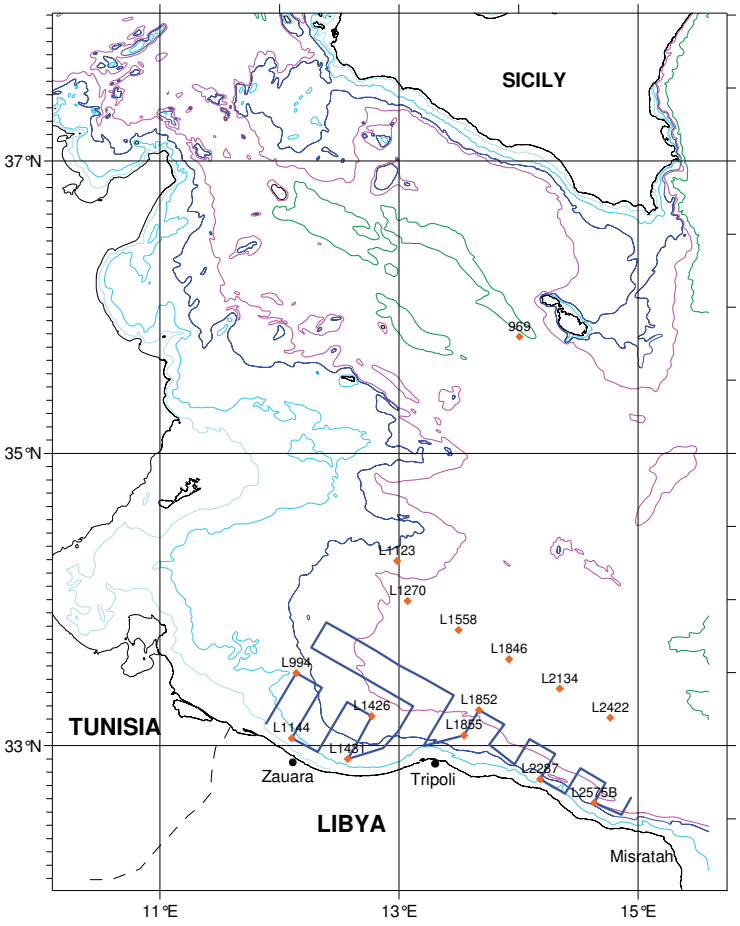

Figure 35. Stations where water samples were collected for the analysis of calcareous micro-algae

6.2 Results

The results of quantitative analyses point out that, in the summer period, the phytoplankton association of Libyan western coast water is generally characterized by abundant diatoms, and dinoflagellates, rare coccolithophyceae and very rare silicoflagellates (see quantitative section and surface maps).

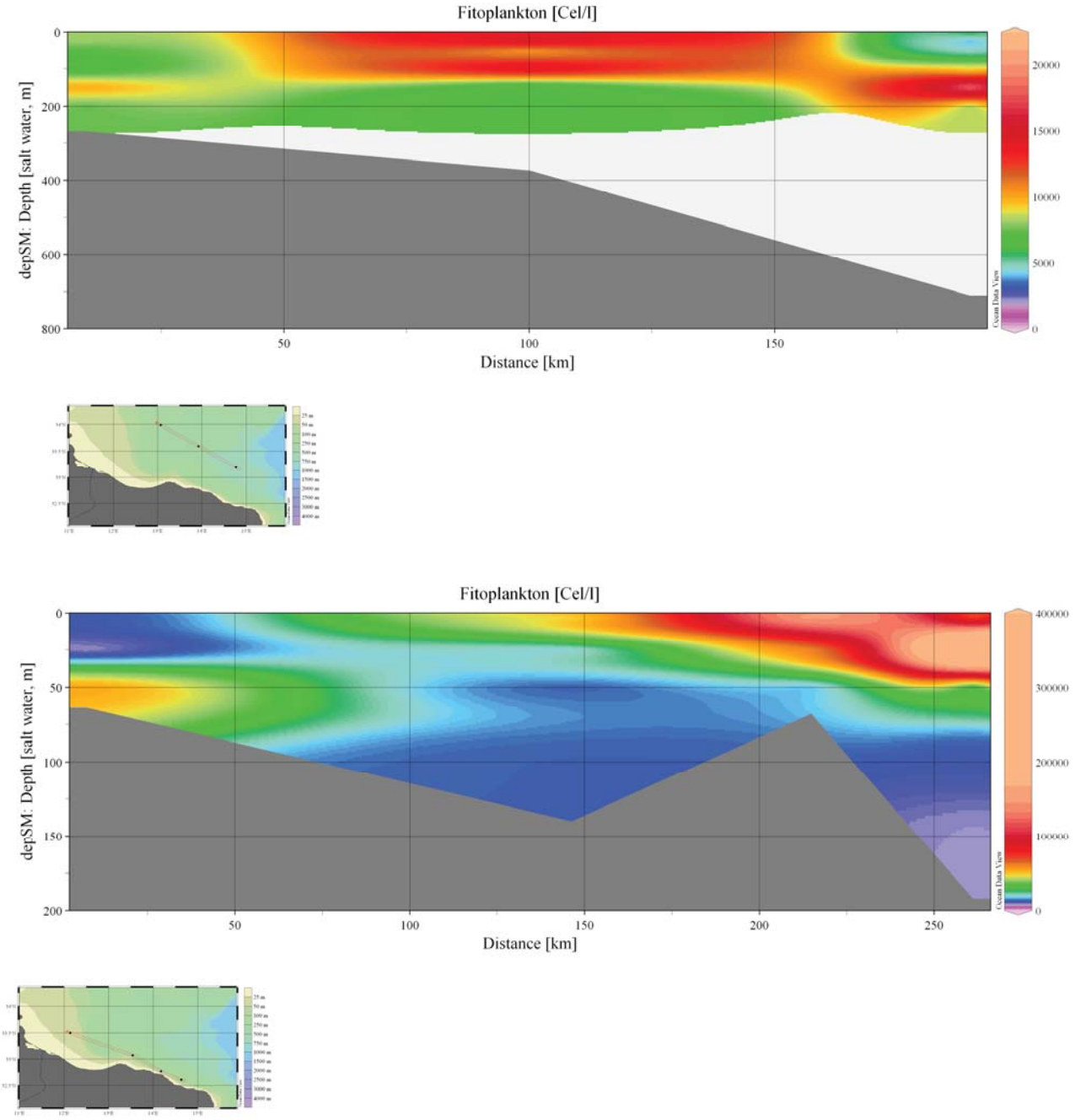

Figure 36. Phytoplankton concentration along 2 transects in the study area.

A very high concentration of phytoplankton is located in the easternmost part of the investigated area, and characterizes the first 100 meters of the water column.

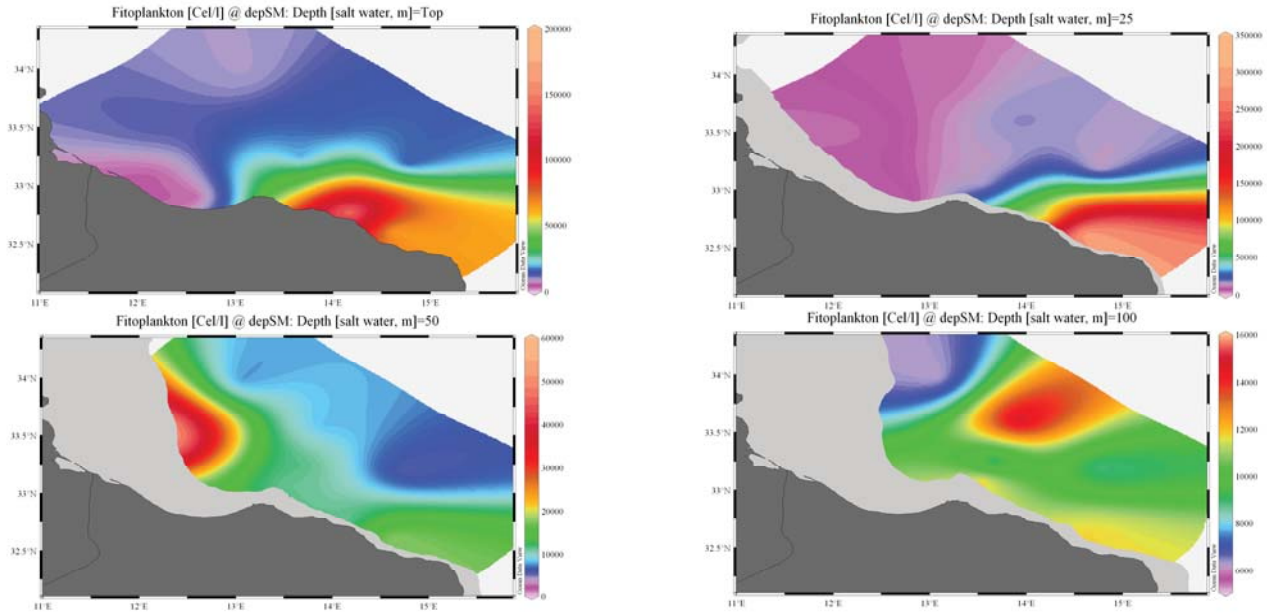

Figure 37. Phytoplankton concentration in the study area at different depths (surface, 25, 50 and 100m).

6.2.1 Dinoflagellates

Dinoflagellates are microscopic, unicellular, flagellated, often photosynthetic protists, commonly regarded as "algae" (Division Dinoflagellata). They are characterized by a transverse flagellum that encircles the body (often in a groove known as the cingulum) and a longitudinal flagellum oriented perpendicular to the transverse flagellum. This imparts a distinctive spiral to their swimming motion. Both flagella are inserted at the same point in the cell wall, by convention defining the ventral surface. This point is usually slightly depressed, and is termed the sulcus. In heterotrophic dinoflagellates this is the point where a conical feeding structure, the peduncle, is projected in order to consume food.

Dinoflagellates possess a unique nuclear structure at some stage of their life cycle a dinokaryotic nucleus (as opposed to eukaryotic or prokaryotic), in which the chromosomes are condensed. The cell wall of many dinoflagellates is divided into plates of cellulose ("armor") within amphiesmal vesicles, known as a theca. These plates form a distinctive geometry/topology known as tabulation, which is the main means for classification.

Both heterotrophic and autotrophic dinoflagellates are known. Some are both. They form a significant part of primary planktonic production in both oceans and lakes. Most dinoflagellates go through moderately complex life cycles involving several steps, both sexual and asexual, motile and non-motile. Some species form cysts composed of sporopollenin (an organic polymer), and preserve as fossils in the sedimentary record. Often the tabulation of the cell wall is somehow expressed in the shape and/or ornamentation of the cyst.

Besides being important primary producers, and therefore an important part of the food chain, dinoflagellates are also known for producing nasty toxins, particularly when they occur in large numbers, called "red tides" because the cells are so abundant they make the water change colour. Besides being bad for a large range of marine life, red tides can also introduce non-fatal or fatal amounts of toxins into animals (particularly shellfish) that may be eaten by humans, who are also affected by the toxins. Many of these toxins are quite potent, and if not

fatal, can still cause neurological and all sorts of other nasty effects. Add this to the rather ominous suspicion that red tides may be more common thanks to human inputs of phosphates and warmer global temperatures, and you can probably see why we have a vested interest in finding out more about them - both medical and economic.

The section showing quantitative distribution with a high values (10000 ~ 3000 cell\l) in the first 25 meters in the westernmost part of the investigated area (probably human settler) and a less abundant concentration in the middle part of investigated transect.

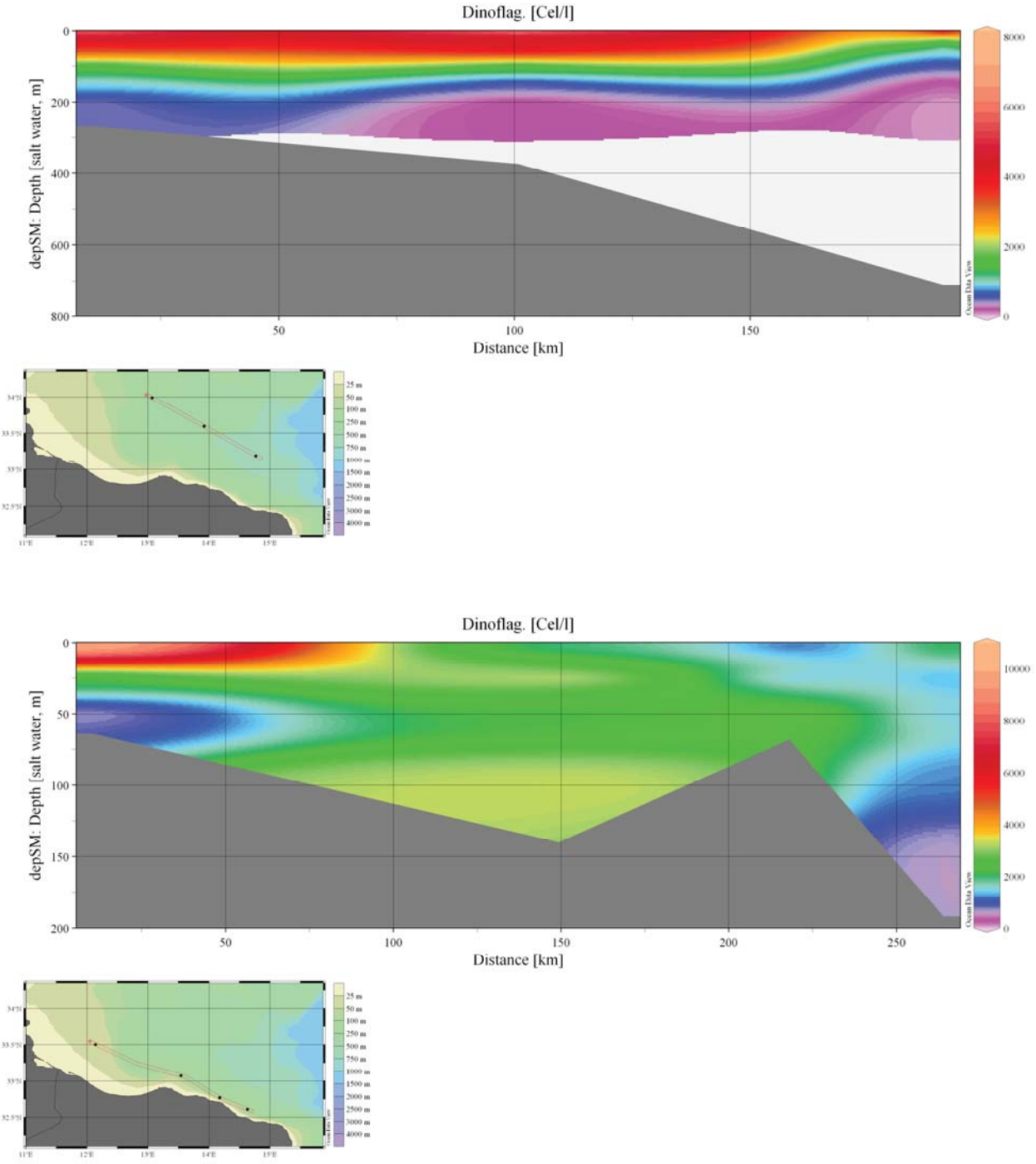

Figure 38. Concentration of dinoflagellates along two transects in the study area.

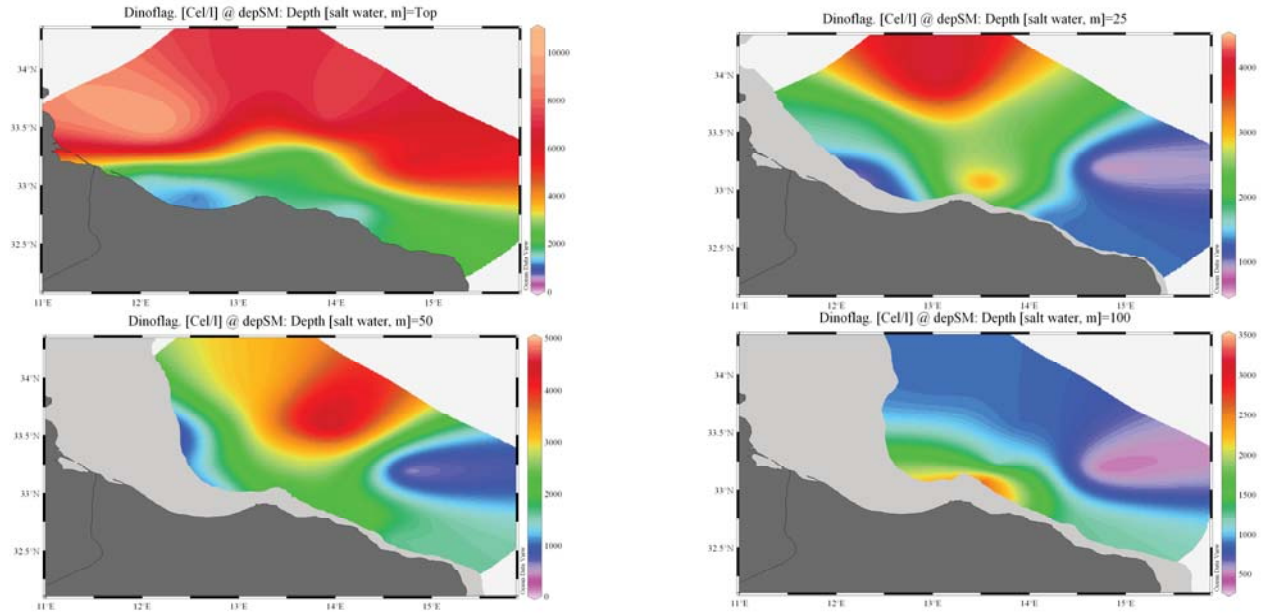

Figure 39. Dinoflagellates concentration in the study area at different depths (surface, 25, 50 and 100m).

6.2.2 Diatoms

Diatoms are photosynthesising algae, they have a siliceous skeleton (frustule) and are found in almost every aquatic environment including fresh and marine waters, soils, in fact almost anywhere moist. They are non-motile, or capable of only limited movement along a substrate by secretion of mucilaginous material along a slit-like groove or channel called a raphe. Being autotrophic they are restricted to the photic zone (water depths down to about 200m depending on clarity). Both benthic and planktic forms exist. Diatoms are formally classified as belonging to the Division Chrysophyta, Class Bacillariophyceae. The Chrysophyta are algae which form endoplasmic cysts, store oils rather than starch, possess a bipartite cell wall and secrete silica at some stage of their life cycle. Diatoms are commonly between 20-200 microns in diameter or length, although sometimes they can be up to 2 millimeters long. The cell may be solitary or colonial (attached by mucous filaments or by bands into long chains). Diatoms may occur in such large numbers and be well preserved enough to form sediments composed almost entirely of diatom frustules (diatomites), these deposits are of economic benefit being used in filters, paints, toothpaste, and many other applications.

Diatoms are divided into two Orders. The Centrales (now called the Biddulphiales) which have valve striae arranged basically in relation to a point, an annulus or a central areola and tend to appear radially symmetrical, and the Pennales (now called Bacillariales) which have valve striae arranged in relation to a line and tend to appear bilaterally symmetrical. The valve face of the diatom frustule is ornamented with pores (areolae), processes, spines, hyaline areas and other distinguishing features. It is these skeletal features which are used to classify and describe diatoms, which is an advantage in terms of palaeontology since the same features are used to define extant species as extinct ones. The classification system developed by Simonsen (1979) and further developed by Round et al. (1990) is currently the most commonly accepted. Diatoms commonly found in the marine plankton may be divided into the centric diatoms including three sub-orders based primarily on the shape of the cells, the polarity and the arrangement of the processes. These are the Coscinodiscineae, with a marginal ring of processes and no polarity to the symmetry, the Rhizosoleniineae with no

marginal ring of processes and unipolar symmetry, and the Biddulphiineae with no marginal ring of processes and bipolar symmetry. The pennate diatoms are divided into two sub-orders, the Fragilariineae which do not posses a raphe (araphid) and the Bacillariineae which posses a raphe.

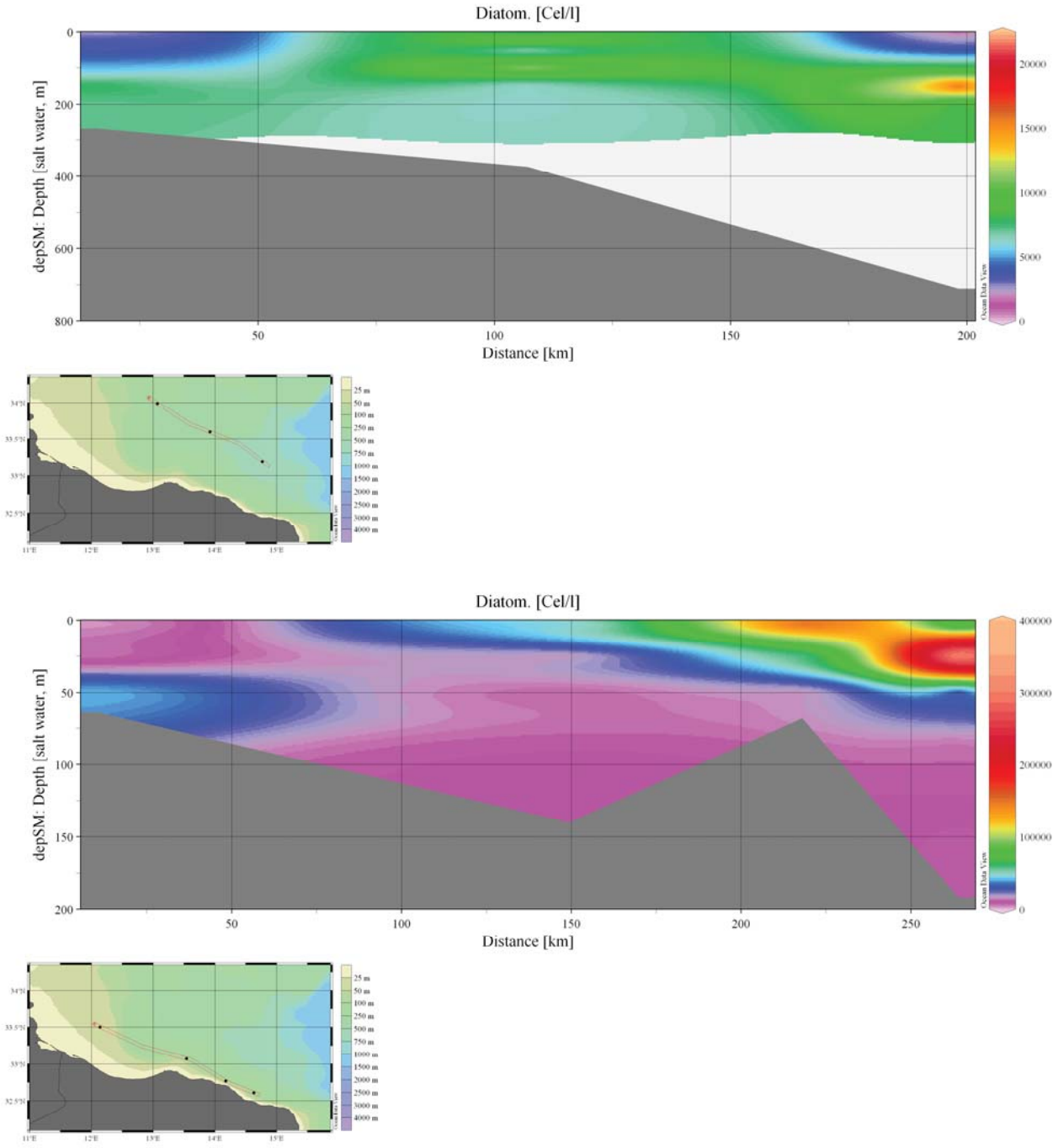

Figure 40. Diatoms concentration along 2 transects in the study area

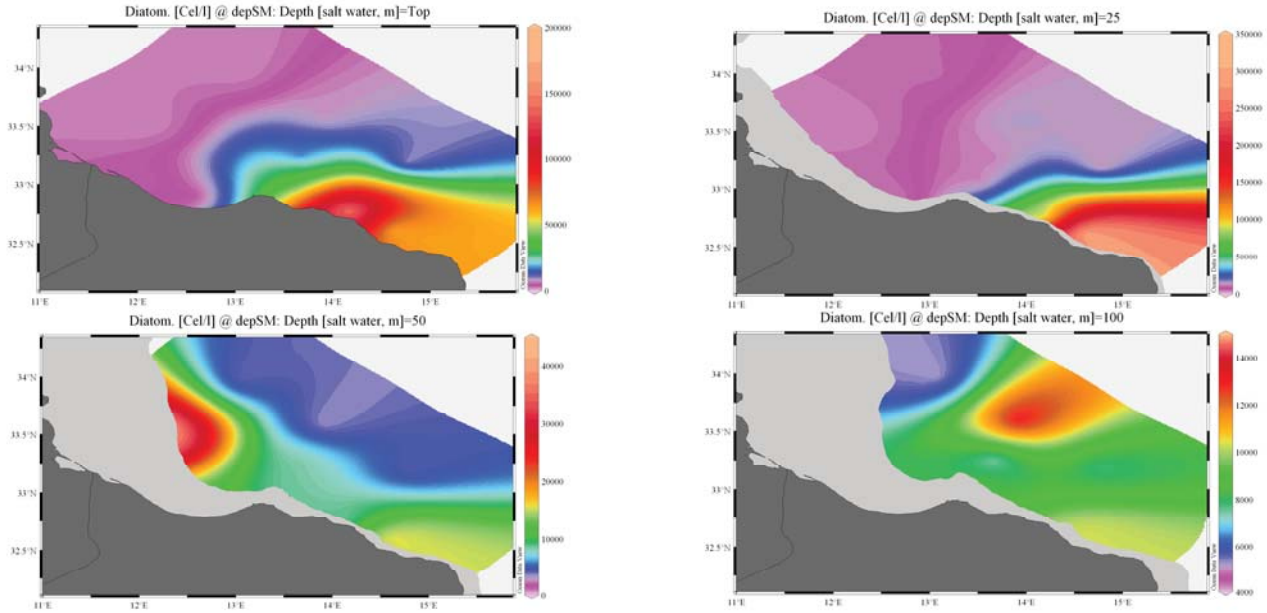

Figure 41. Diatoms concentration in the study area at different depths (surface, 25, 50 and 100m).

Diatoms have been well studied both in their natural habitat and in cultures by biologists and there is therefore a wealth of knowledge on their biology and ecology. The protoplast of diatoms consists of a cytoplasmic layer that lines the interior of the frustule and surrounds a large central vacuole, within the cytoplasmic layer there is a diploid nucleus and two to several pigment-bearing plastids (the site of photosyntheseis). The diatom frustule is often likened to a pill-box or agar dish with an epitheca (larger upper valve), and a hypotheca (smaller lower valve). The vertical lip or rim of the epitheca is called the epicingulum, and the epicingulum fits over (slightly overlaps) the hypocingulum of the hypotheca. The epicingulum and hypocingulum with one or several connective bands make up the girdle. Many diatoms are heterovalvate, i.e., the two valves of the frustule are dissimilar. This is most obvious within the family Achnanthaceae where one valve has a raphe and the other does not, and the Cymatosiraceae where one valve has a tubular process and the other does not. Chain-forming species with cells linked together by siliceous structures may, in addition, have separation valves. These valves are morphologically different from the valves within the chain. Therefore, one species may have four morphologically distinct types of valves.

The section showing quantitative distribution with a very high values (400000 ~ 50000 cell\l) in the first 75 meters in the easternmost part of the investigated area and, below 50 meters, a less abundant concentration in the westernmost part of investigated transect. In generally diatoms are the dominant phytoplankton compound of the Libya western coast.

6.2.3 Coccolithophores

Like any other type of phytoplankton, coccolithophores are one-celled marine plants that live in large numbers throughout the upper layers of the ocean. Unlike any other plant in the ocean, coccolithophores surround themselves with a microscopic plating made of limestone (calcite). These scales, known as coccoliths, are shaped like hubcaps and are only three one-thousandths of a millimeter in diameter.

What coccoliths lack in size they make up in volume. At any one time a single coccolithophore is attached to or surrounded by scales. Additional coccoliths are dumped into

the water when the coccolithophores multiply asexually or die. In areas with trillions of coccolithophores, the waters will turn an opaque turquoise from the dense cloud of coccoliths. It's estimate that the organisms dump more than 1.5 million tons (1.4 billion kilograms) of calcite a year, making them the leading calcite producers in the ocean.

Most phytoplankton needs both sunlight and nutrients from deep in the ocean. The ideal place for them is on the surface of the ocean in an area where plenty of cooler, nutrient-carrying water is upwelling from below. In contrast, the coccolithophores prefer to live on the surface in still, nutrient-poor water in mild temperatures.

Coccolithophores do not compete well with other phytoplankton. Yet unlike their cousins, coccolithophores do not need a constant influx of fresh food to live. They often thrive in areas where their competitors are starving. Typically, once they are in a region, they dominate and become more than 90 percent of the phytoplankton in the area.

Coccolithophores live mostly in subpolar regions. Some other places where blooms occur regularly are the northern coast of Australia and the waters surrounding Iceland. In the past two years, large blooms of coccolithophores have covered areas of the Bering Sea. This surprises many scientists since the Bering Sea is normally a nutrient-rich body of water.

What do they do to the environment? Coccoliths are not normally harmful to other marine life in the ocean. The nutrient-poor conditions that allow the coccolithophores to exist will often kill off much of the larger phytoplankton. Many of the smaller fish and zooplankton that eat normal phytoplankton also feast on the coccolithophores. In nutrient-poor areas where other phytoplankton are scarce, the coccolithophores are a welcome source of nutrition.

In the long term, the plants seem to be good for the environment. Coccolithophores make their coccoliths out of one part carbon, one part calcium and three parts oxygen ($CaCO_3$). So each time a molecule of coccolith is made, one less carbon atom is allowed to roam freely in the world to form greenhouse gases and contribute to global warming. Three hundred twenty pounds of carbon go into every ton of coccoliths produced. All of this material sinks harmlessly to the bottom of the ocean to form sediment.

The coccolithophores' short-term effect on the environment is somewhat more complex. This effect again has to do with the formation of their coccoliths and the chemical reaction involved in the process. The chemical reaction that makes the coccolith also generates a carbon dioxide molecule, a potent greenhouse gas, from the oxygen and carbon already in the ocean. While much of the gas is sucked back in by the coccoliths (all plants take in carbon dioxide for food) some of it escapes into the atmosphere and immediately becomes part of the greenhouse gas problem. Scientists are concerned in the short term that greenhouse gases will cause the upper layers of the ocean to become more temperate and stagnant. This would increase the number of coccoliths in the world, which would produce more greenhouse gas.

The coccolithophores also affect the global climate in the short term by increasing the oceans' albedo. Albedo is the fraction of sunlight an object reflects--higher albedo values indicate more reflected light. Coccolithophore blooms reflect nearly all the visible light that hits them. Since most of this light is being reflected, less of it is being absorbed by the ocean and stored as heat.

The section show quantitative distribution with a gradually increase values (500 ~ 14000 cell\l) in the first 100 meters of the western-central part of the investigated area. In the

central–estern part the calcareous plankton rapidly decrease in abundance, never overcome 400 cell/l density.

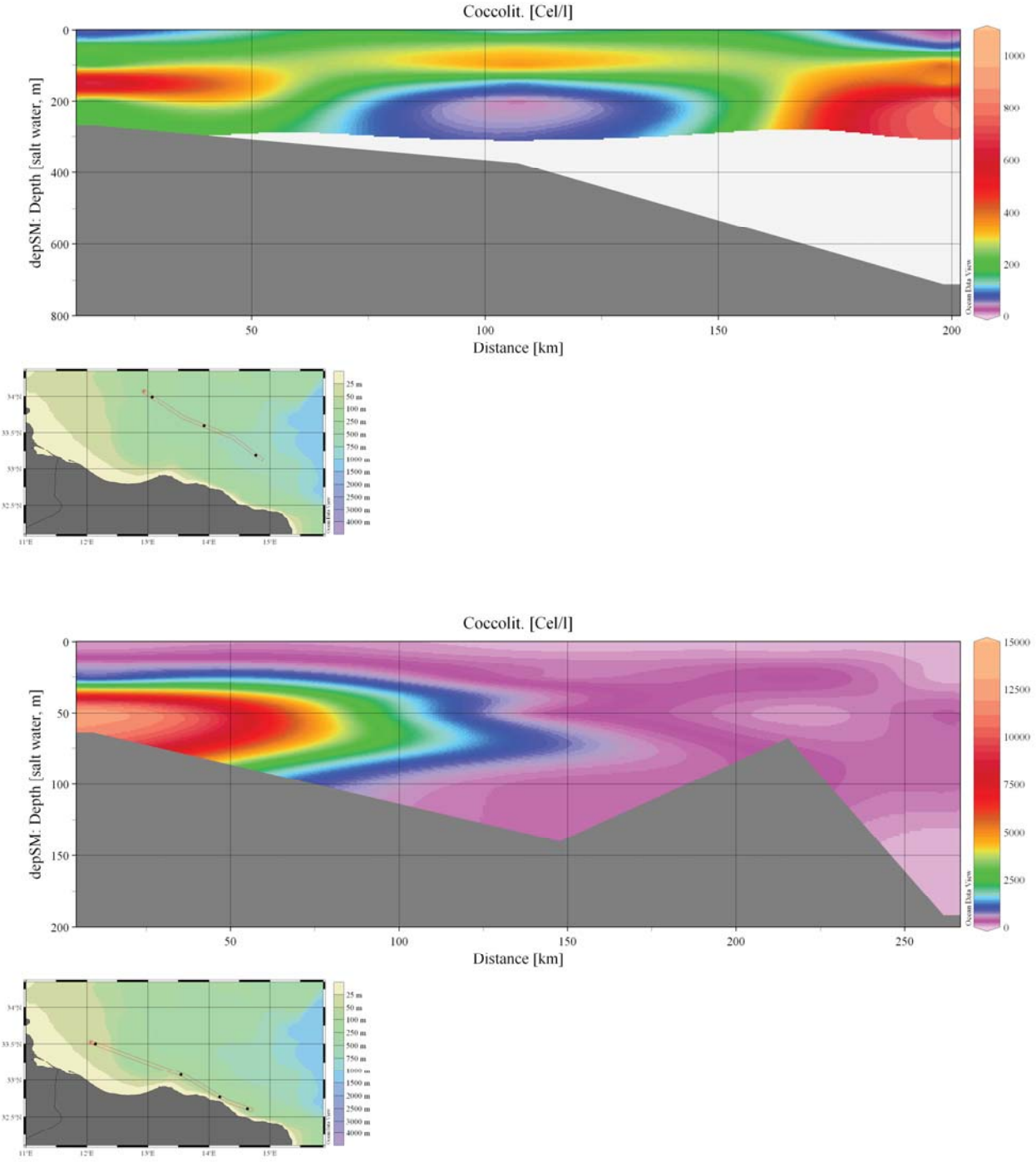

Figure 42. Coccolithophores concentration along 2 transects in the study area

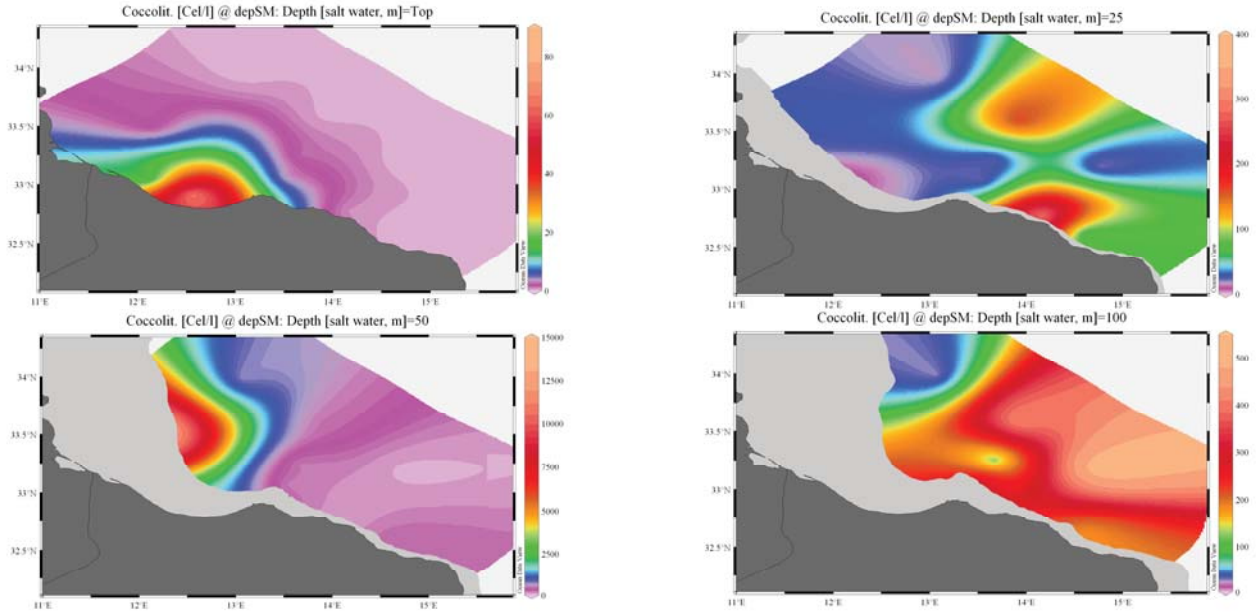

Figure 43. Coccolithophores concentration in the study area at different depths (surface, 25, 50 and 100m).

6.2.4 Silicoflagellates

Silicoflagellates are a small group of unicellular heterokont algae, found in marine environments. In one stage of their life cycle, they produce a siliceous skeleton, composed of a network of bars and spikes arranged to form an internal basket. These form a small component of marine sediments, and are known as microfossils from as far back as the early Cretaceous. There is one living genus, *Dictyocha*, with two commonly recognized species. There are also several extinct genera, but their classification is difficult, since skeletons may show diverse forms within each living species. *Dictyocha* has one golden-brown chloroplast and a long flagellum extended into a wing-like shape. The skeleton-bearing stage is uninucleate, with many microtubule-supported projections, and there are also uninucleate and micronucleate stages that do not produce skeletons, but how they relate to each other is poorly understood. The cell structure places the silicoflagellates in a group called the axodines. They are usually treated as an order, called the Dictyochales by botanists and the Silicoflagellida by zoologists.

Like the diatoms, the silicoflagellates are especially abundant in areas of upwelling and in equatorial waters but are also abundant at high latitudes. Silicoflagellates skeletons usually comprise 1-2% of the siliceous component of marine sediments; they are thus much less abundant than diatoms. However, they are widely distributed throughout the world ocean.

The sections show, as expected, quantitative distribution with very low values located in the deeper westernmost (-50 meters) and central (-150 meters) part of the investigated area. The recognized assemblage is constituted only by *Dictyocha fibula* specimens that never overcome 400 cell/l density.

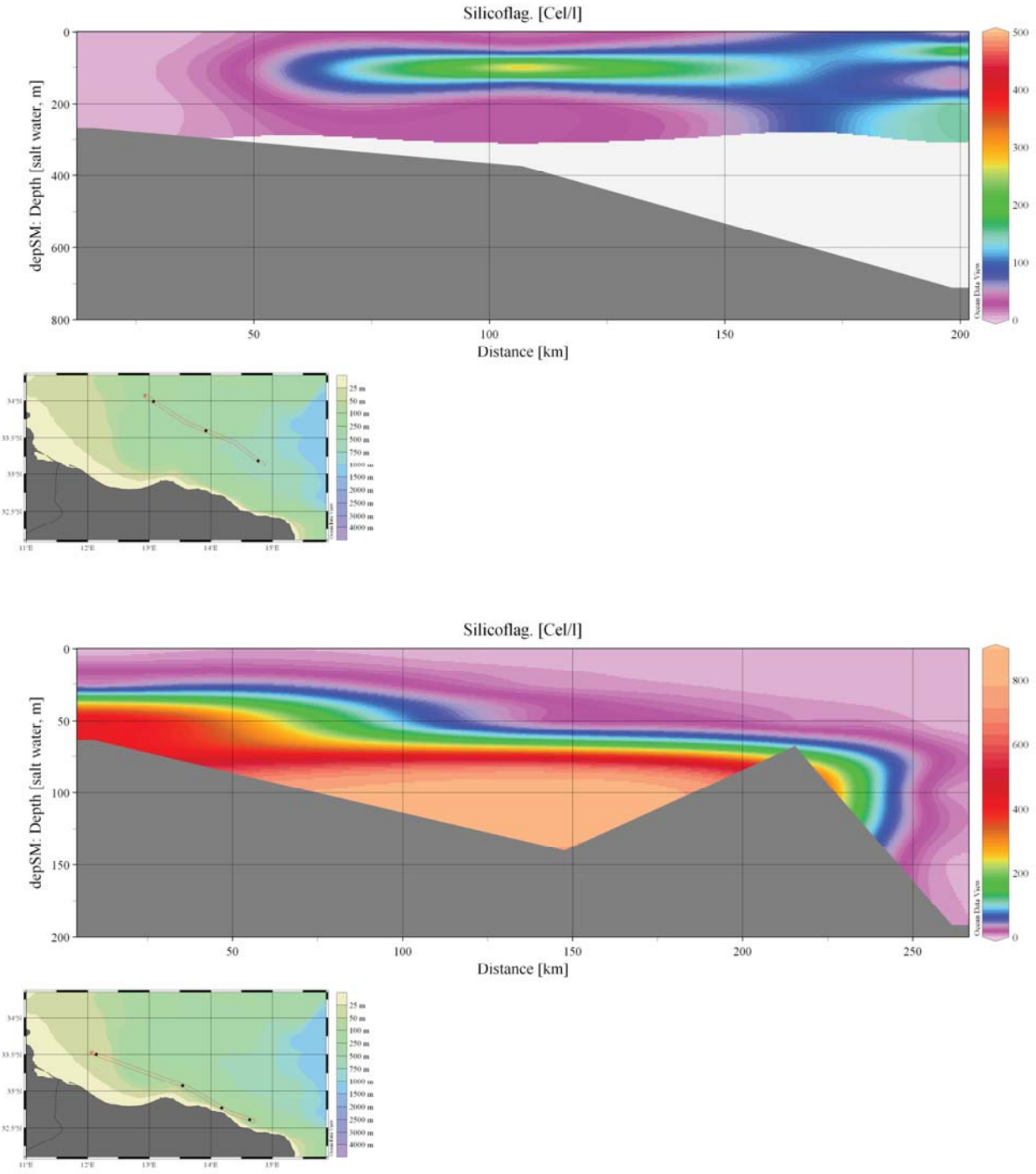

Figure 44. Silicoflagellates concentration along 2 transects in the study area

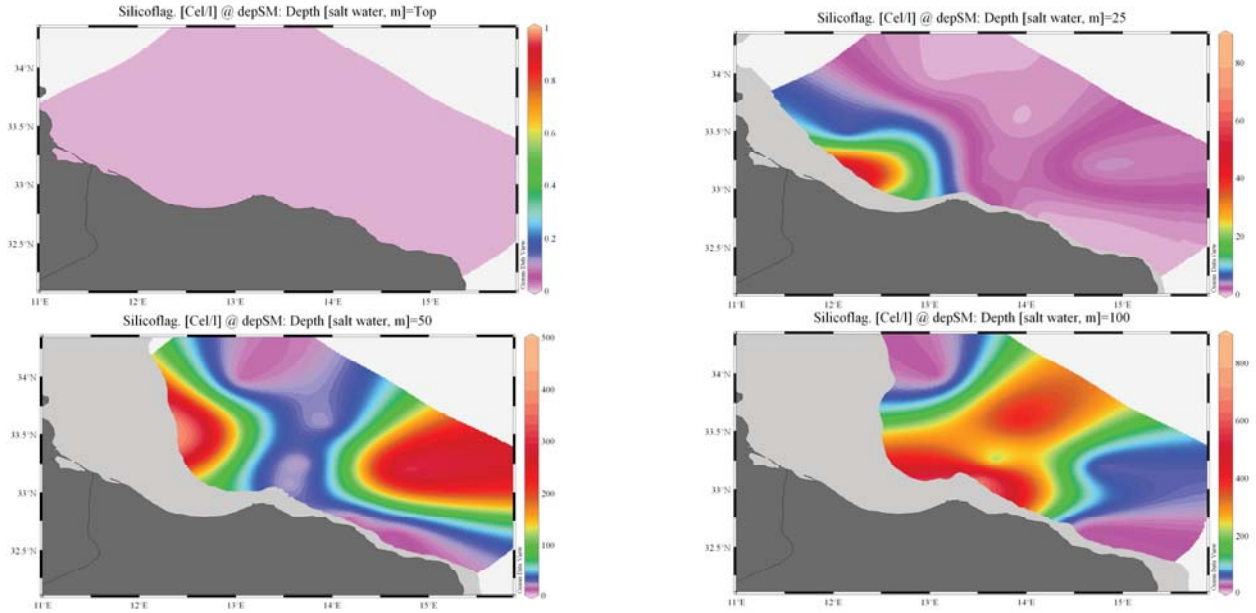

Figure 45. Silicoflagellates concentration in the study area at different depths (surface, 25, 50 and 100m)

6.2.5 Calcareous nanofossil surface sediment assemblages from the Sicily Channel (central Mediterranean Sea): palaeoceanographic implications

Quantitative analysis on 67 calcareous nannofossil assemblages of surface sediments recovered in a wide area across the Sicily Channel has been carried out in order to improve the interpretation of palaeontological data based on this planktonic group in a key area for Mediterranean palaeoceanographic studies. The investigation focused on three case studies that demonstrate the high potentiality of such a combined approach, taking into account the recent distribution of taxa or groups of taxa on the sea floor and the palaeontological record. The distribution of reworked specimens over the northern Sicily Channel sea floor validates the role of southern Sicily as a source region for reworked nannofossils and the role of rivers as their carrier. Eustatic sea-level fluctuations can be considered to be the main factor that influenced the abundance of variations in sedimentary sequences of this area. The distribution of *Florisphaera profunda* (Figure 46) can be explained in terms of topography (positive correlation) and mesoscale oceanographic circulation. In particular, its significant anti-correlation to the amount of chlorophyll-A deduced by satellite imagery validates the use of this species as a proxy for palaeoproductivity reconstructions. Finally, high abundance values of *G. oceanica* are confined to the westernmost part of the Sicily Channel, coinciding with a water mass salinity minimum. In particular, abundances of up to about 10% were observed in the westernmost part of the African Margin, suggesting the importance of the Atlantic Tunisian Current, whose activity is more pronounced in winter. The comparison of data of this species between 135 and 110 kyr BP, inside and outside the Channel, led us to deduce that the physical transport on almost unmodified waters of Atlantic origin might be the most important factor for its significant occurrence.

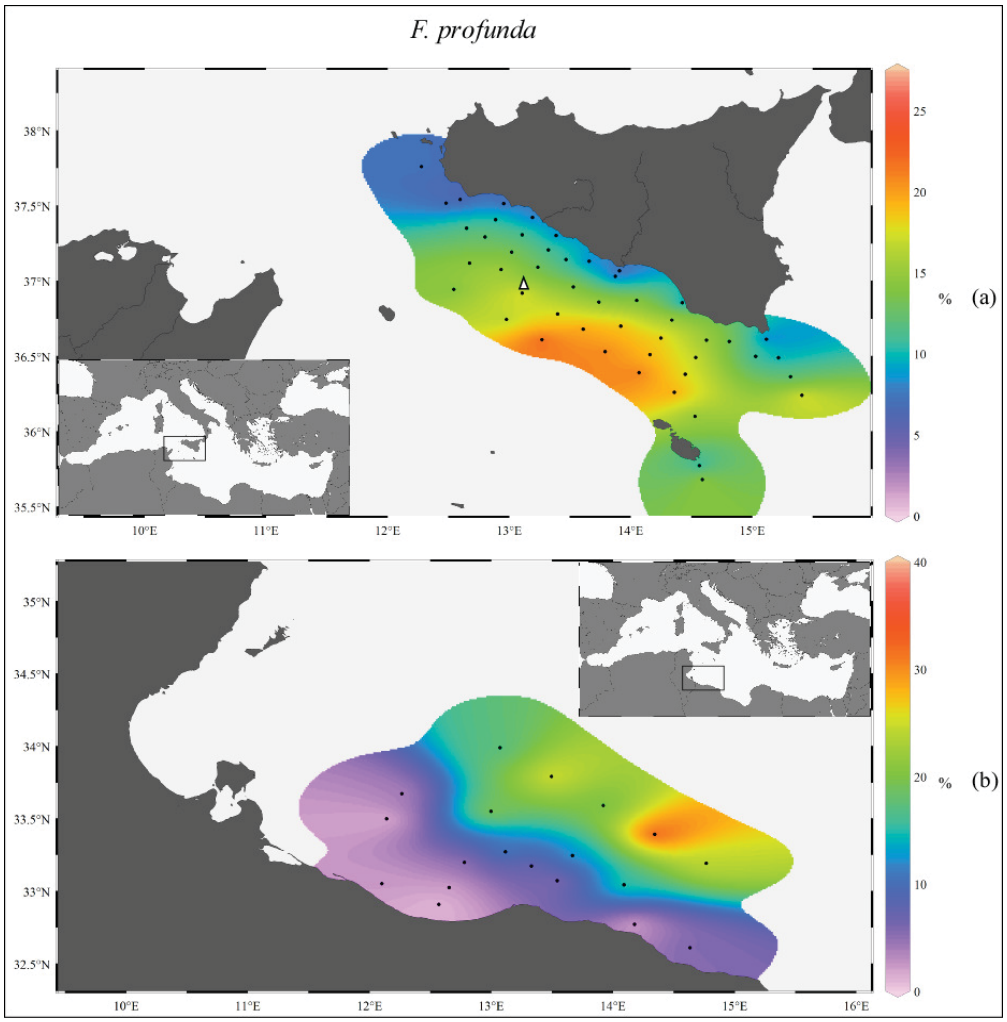

Figure 46. Box Corer quantitative distribution map of *Florisphaera profunda*.

7 Organic matters

The trophic status of the waters is here described by means of nutrients and suspended matter, both quantitative and trophic parameters.

7.1 Material and methods

During the MedSudMed-06 survey, 74 water samples were collected from different depth levels of water column (5, 25, 50, 100, 150, 200, 500, bottom) in 14 stations located in the western Libyan sea area. Samples of waters were collected with Niskin bottles for the analysis of POC (Particulate Organic Carbon) and PON (Particulate Organic Nitrogen) concentration. Sampling stations were chosen along transects perpendicular to the coast; the sampling design was then adapted according to the time available, forbidden areas etc. (Figure 47).

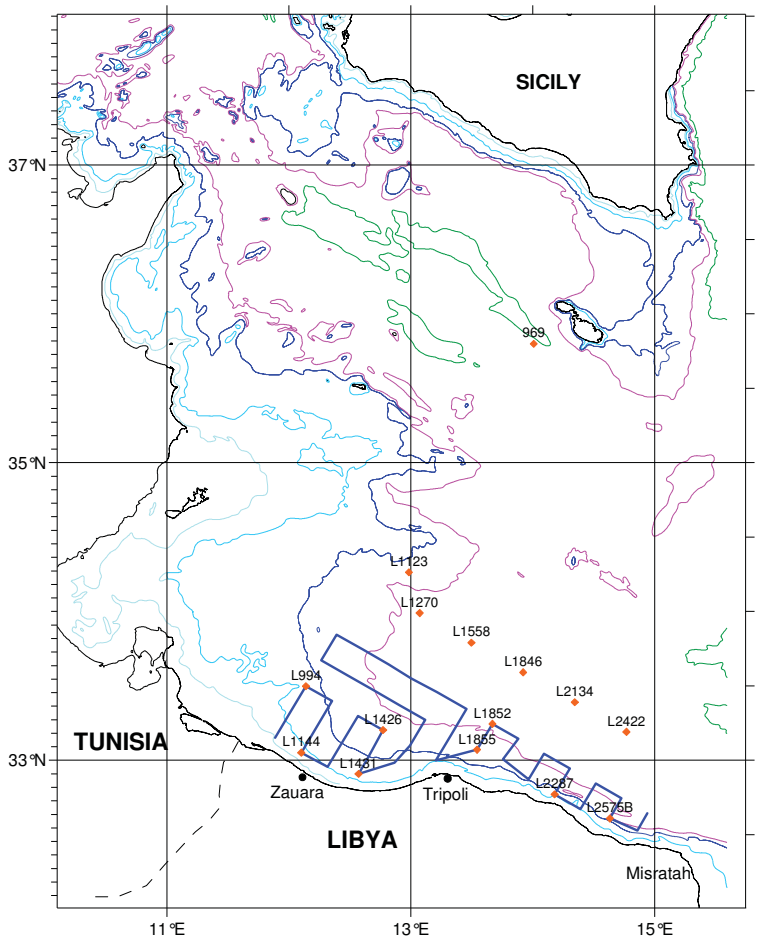

Figure 47. **Position of stations where samples of water were collected for the POC, PON and nutrients analysis.**

For TSM (Total Suspended Matter), POC (Particulate Organic Carbon) and PON (Particulate Organic Nitrogen) measurements, suitable quantities of water samples (1000 ml) were beforehand screened through a 200 µm net to remove larger zooplankton, and then filtered on precombusted (450 °C, 4^h) and pre-weighted Whatman GF/F filters (0.75 µm pore size). After filtering, the samples collected on filters were dried (60 °C, 12^h) and weighted to calculate the TSM incidence. Subsequently, the filters were exposed to hydrochloric acid fumes for 6^h at room temperature (Iseki et al., 1987), to destroy the inorganic carbon, then were dried (60 °C, 12^h) and rolled into tin discs. Finally POC and PON analyses were performed by a Perkin-Elmer CHN Elemental Analyser (Mod. 2400) at a combustion temperature of 980 °C, using Acetanilide as standard.

7.2 Results and discussion

The estimated values of TSM, POC and PON are reported in Table 2. High levels of Total Suspended Matter (TSM) were found in all the analyzed samples, ranging from 7.60 mg/l to 19.65 mg/l. No significant correlation was found between TSM and POC values (; r = 0.328). However, the TSM values were higher in the western part of the investigated area, where the POC showed very low incidence, in both 5 m and 25 m layers

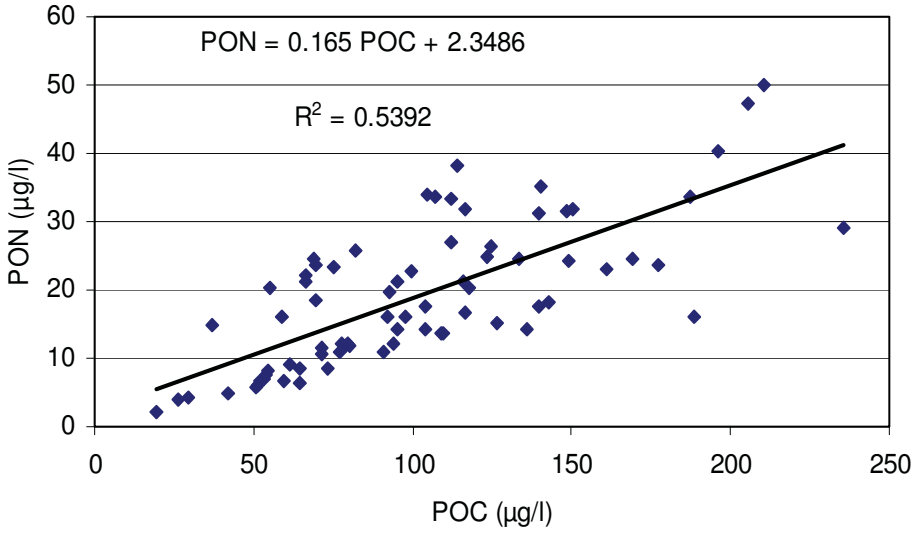

Figure 48. **Correlation between Particulate Organic Carbon and Particulate Organic Nitrogen.**

There was a significant positive correlation between POC and PON values (Figure 48; r = 0.734). Notably, the POC and PON values were not particularly high, but higher than those we had found in our previous investigations in the Sicily Channel. The highest POC values (>150µgC/l) were recorded in the euphotic layer (max = 235.60 µg/l at St. 2575) for the off shore area, while in the near shore they were generally lower.

The C/N ratio values show a general condition of equilibrium between the trophic components (autotrophy, heterotrophy, detritus). In particular, a good efficiency level of the autotrophic compartment was find in the eastern area, where C/N values ranged between 6 and 8. On the contrary, in the Zauara area the C/N values lover than 5 indicate the prevalence of heterotrophic activities. However, in the off shore area in front of Tripoli, higher C/N ratio values suggest that the phytoplankton community is not very efficient or little stressed (C/N between 8 and 10). Here detritus resulted occasionally prevailing over the biotic constituents (C/N >10).

Table 2. Estimated values of Total Suspended Matter (TSM), Particulate Organic Carbon (POC) and Particulate Organic Nitrogen (PON).

Station	Depth	NO_3 µM	NH_4 µM	PO_4 µM	TSM mg/l	POC µg/l	PON µg/l	C/N
L1144	-5	0.33	4.68	0.78	10.57	135.9	14.3	9.50
L1144	-25	0.47	0.77	0.42	10.98	142.7	18.1	7.88
L1431	-5	0.74	0.35	0.08	10.13	104	17.5	5.94
L1431	-25	1.66	1.07	0.50	16.89	29.4	4.3	6.84
L1431	-60	1.62	0.21	0.10	10.00	103.7	14.3	7.25
L1855	-5	1.46	0.48	0.68	13.22	59.70	6.60	9.05
L1855	-25	2.02	1.17	0.24	13.09	51.70	6.80	7.60
L1855	-50	2.13	0.96	0.01	8.43	61.40	9.10	6.75
L1855	-100	2.05	0.20	0.55	9.54	79.60	12.20	6.52
L1855	-140	3.83	0.22	0.19	10.19	73.60	8.40	8.76
L2287	-5	0.02	0.88	0.45	10.96	109.30	13.70	7.98
L2287	-25	0.01	0.62	0.51	11.16	139.50	17.70	7.88
L2287	-50	0.43	0.51	0.35	10.82	97.80	16.20	6.04
L2575b	-5	1.38	1.88	0.10	12.85	235.60	29.00	8.12
L2575b	-25	1.32	0.87	0.32	13.29	76.90	10.80	7.12
L2575b	-50	1.05	0.78	0.45	10.51	160.80	22.90	7.02
L2575b	-100	0.98	0.51	0.58	10.81	116.40	16.80	6.93
L2575b	-150	2.97	0.28	0.16	11.46	64.30	8.50	7.56
L2575b	-200	1.77	0.75	0.25	12.08	53.10	7.00	7.59
L994	-5	0.46	1.07	0.39	19.95	95.00	14.30	6.64
L994	-25	0.02	1.43	0.32	11.63	78.70	11.80	6.67
L994	-50	1.00	1.11	0.65	12.94	71.30	11.50	6.20
L1426	-5	0.19	0.53	0.03	15.59	82.30	25.80	3.19
L1426	-25	0.25	0.74	0.55	19.06	69.00	24.50	2.82
L1426	-50	0.16	0.61	0.58	13.06	69.80	23.70	2.95
L1426	100	0.99	1.19	0.01	11.77	112.10	33.40	3.36
L1426	150	1.88	1.38	0.63	13.26	66.7	22.00	3.03
L1852	-5	0.19	0.53	0.03	11.69	51.50	6.10	8.44
L1852	-25	0.25	0.74	0.55	11.33	50.80	5.90	8.61
L1852	-50	0.16	0.61	0.58	10.63	77.70	12.00	6.48
L1852	-100	0.99	1.19	0.01	10.3	54.60	8.20	6.66
L1852	-150	1.88	1.38	0.63	11.95	91.00	10.80	8.43
L1123	-5	0.82	0.97	0.69	9.47	196.3	40.4	4.86
L1123	-25	0.50	1.06	0.56	9.97	104.9	33.9	3.09
L1123	-50	0.08	0.42	0.63	11.03	116.4	31.7	3.67
L1123	-100	0.69	0.40	0.56	16.29	114.2	38.1	3.00
L1123	-125		0.38	0.36	10.42	107.3	33.6	3.19
L1270	-5	0.48	0.21	0.47	12.58	140.3	35.1	4.00
L1270	-25	0.28	0.38	0.54	10.79	148.3	31.5	4.71
L1270	-50	0.01	0.12	0.43	9.71	139.9	31.1	4.50
L1270	-100	0.69	0.28	0.51	10.22	150.2	31.9	4.71
L1270	-150	0.42	0.19	0.45	10.80	99.4	22.6	4.40
L1270	-200	0.91	0.11	0.61	12.35	112.2	27.0	4.16
L1270	-270	0.87	0.20	0.13	11.14	95.0	21.1	4.50
L1558	0	0.56	0.64	0.34	10.79	58.9	16.0	3.68
L1558	-25	0.98	1.61	0.33	8.46	187.5	33.7	5.56
L1558	-50	1.13	0.62	0.32	9.41	133.4	24.5	5.44
L1558	-100	1.36	0.41	0.08	8.81	124.5	26.4	4.72

Station	Depth	NO_3 µM	NH_4 µM	PO_4 µM	TSM mg/l	POC µg/l	PON µg/l	C/N
L1558	-150	2.11	0.81	0.37	12.50	37.1	1 4.9	2.49
L1558	-200	2.15	0.24	0.48	10.27	118.0	20.2	5.84
L1558	-339	1.93	0.29	0.30	11.39	149.0	24.1	6.18
L1846	-5	1.43	0.19	0.37	8.83	188.5	16.0	11.78
L1846	-25	1.58	0.19	0.55	8.42	169.1	24.4	6.93
L1846	-50	0.02	0.26	0.33	7.60	126.6	15.2	8.33
L1846	-100	2.02	0.29	0.22	12.22	93.8	12.2	7.69
L1846	-150	0.93	0.51	0.45	9.84	64.8	6.4	10.13
L1846	-200	1.41	0.30	0.26	12.55	19.7	2.1	9.38
L1846	-375	1.37	0.46	0.45	12.28	53.9	7.6	7.09
L2134	0	1.20	0.20	0.14	10.56	71.7	10.5	6.83
L2134	-25	1.00	0.52	0.42	9.25	177.6	23.6	7.53
L2134	-50	1.09	0.36	0.29	9.31	109.7	13.7	8.01
L2134	-100	1.42	0.45	0.05	10.78	115.8	21.2	5.46
L2134	-150	2.27	0.32	0.19	10.56	42.1	4.8	8.81
L2134	-200	3.11	0.67	0.43	9.56	80.2	11.8	6.80
L2134	-500	3.60	0.58	0.53	10.35	92.0	16.0	5.75
L2134	-605	5.47	0.34	0.52	10.29	26.4	3.8	6.95
L2422	-5	1.07	0.18	0.37	12.95	66.5	21.1	3.15
L2422	-25	0.71	0.43	0.43	11.03	205.8	47.2	4.36
L2422	-50	0.76	0.44	0.09	10.89	123.5	24.9	4.96
L2422	-100	1.62	0.55	0.13	10.21	210.6	50.0	4.21
L2422	-150	1.76	0.16	0.34	10.35	69.5	18.5	3.76
L2422	-200	1.15	0.40	0.12	12.98	55.4	20.2	2.74
L2422	-500	5.19	0.50	0.35	12.86	75.4	23.4	3.22
L2422	-700	6.08	0.44	0.26	10.25	92.8	19.6	4.73

8 Nutrients

8.1 Material and methods

Water samples for ammonia (NH_4), nitrite + nitrate (NO_2+NO_3) and orthophosphate (PO_4) were filtered through a Millipore 0.45-micron membrane filter, into 50 ml sample vials and kept frozen (-20° C). NH_4 concentration was estimated using the Aminot and Chaussepied method (1983), while the other nutrients were estimated according to Strickland and Parsons method (1972). Inorganic nutrient concentrations were determined by the Varian spectrophotometer (Mod. Cary 50).
In the following some detail on the adopted procedure are reported.

a. Nitrite + Nitrate

- **Method description:** The nitrate present in the sample is reduced to nitrite in a coppered cadmium column, in a buffered medium. The nitrites formed and the ones already present in the sample, react with sulphanilamide and N-(1-naphtyl) ethylendiamine in acid medium to give a colored diazonium salt, which is measured at 543 nm. Strickland e Parsons (1972).

- **Reagents:** The washing water was deionized water.
    - The sulphanilamide (SAA) reagent was sulphanilamide 5 g, concentrated hydrochloric acid 50 ml, distilled water q. s. 250 ml.

- The naphtylethylendiamine (NED) reagent was N-(1-naphtyl) ethylendiamine x 2 HCl 0.5 g, distilled water q. s. 500 ml. Buffer solution was EDTA- 4Na 38 g, concentrated hydrochloric acid 1 ml, water q. s. 1000 ml.

- **Standard solutions:** The standard stock (solution A) was KNO3 1.02 g, chloroform 10 drops, water q.s.1000 ml. One ml of solution A when diluted to 200 ml of water gives a working standard of 50 µM/l nitrate (solution B). 1 ml of solution B when diluted to 50 ml of natural low nutrient seawater (LNSW) gives a working standard of 1 µM/l NO3 as N.

b. Orthophosphate

- **Method description:** The orthophosphate present in the sample reacts with molybdate in an acid medium to form phosphomolybdate, and then with ascorbic acid to form molybdenum blue, whose intensity is measured at 880 nm. Strickland e Parsons (1972).

- **Reagents**
  - The molybdate reagent was antimony potassium tartrate 0.136 g, ammonium heptamolybdate tetrahydrate 6 g, concentrated sulphuric acid 27 ml, water q.s.500 ml.
  - The ascorbic acid reagent was ascorbic acid 1.08 g, water q.s. 100 ml.

- **Standard solutions:** The standard stock PO4 as P (solution A) was potassium hydrogen phosphate anhydrous 0.8160 g, chloroform 10 drops, water q.s.1000 ml. One ml of solution A when diluted to 500 ml of water gives a working standard of standard 0.012 µM phosphate (solution B). 1 ml of solution B when diluted to 50 ml of natural low nutrient seawater (LNSW) gives a working standard of 0.24 µM/l PO4 as P.

c. Ammonium

- **Method description:** The ammonia ions present in the sample react with phenol and hypochlorite in an alkaline medium according to Bethelot's reaction; trisodium citrate and EDTA are added to the sample to avoid the precipitation of alkaline hydroxides, while nitroprusside acts as a catalyst. The indophenol blue is measured at 640 nm. Aminot A. e Chaussepied M. (1983).

- **Reagents:**
  - The phenol reagent was phenol, solid and colourless 17.5 g, sodium nitroprusside 0.2 g water q.s.500 ml .
  - The complexing agent for seawater was trisodium citrate, dihydrate 140 g, sodium hydroxide 11 g, trione 11 g, water q.s.500 ml.

- **Standard solutions:** The standard stock NH3 as N (solution A) was ammonium sulphate anhydrous 0.100 g, chloroform10 drops, water q.s.1000 ml. One ml of solution A when diluted to 500 ml of water gives a working standard of 0.003 µM ammonia (solution B). 5 ml of solution B when diluted to 50 ml of natural low nutrient seawater (LNSW) gives a working standard of 0.3 µM/l NH3 as N.

8.2 Results

The estimated values of nutrients for all the analyzed stations in the Libyan waters are reported in Table 2. Surface (0 – 25 m) concentrations of nitrate were high (~ 1.5 µM) in the transect south-north and in the St. 1431 (> 1.5 µM 25-60 m) near Zauara. The vertical values of dissolved nitrate (1.48 ± 1.32 µM) showed an increase with depth (max 6.08 µM, St. 2422 - 700 m) (Table 2).

Nitrate and ammonia generally showed, as expected, opposite trends both at 5m and 25m (NH_4 0.58 ± 0.61 µM/l), in agreement with the recycling of nitrogenous respective compounds. The maximum value of ammonia (4.68 µM/l) was found in surface (5 m) at the station L1144 (Zauara).

The values of reactive phosphate showed a increase in surface layer (5 m) in the south-north Zauara transect (St. L1144, L994 and L1123), and at L1855 and L1852 stations in front of Tripoli (~ 0.6 µM/l). Irregularity in the vertical distribution appeared at several stations (PO_4 = 0.38 ± 0.19 µM/l).

The results show that in the investigated area there is not a clear evidence of dystrophy or pollution events, even if in the Zauara coastal area there are phosphorous and ammonia increments, probably due to human and urban discharges (detergents and sewage). On the other hand, the relatively high nitrate concentration in the coastal Tripoli area can be interpreted as a possible consequence of intensive agriculture and/or use of nitrogen fertilizers.

In conclusion a better trophic equilibrium and a more efficient autotrophic community were found in the eastern zone of the investigate area, where also the nutrients budget is enough to support the activities of the primary compartment. However in the western area, between Zauara and Tripoli, the trophic balance appears shifted through the degradation processes.

9 Trace elements

Samples of waters were collected with Niskin bottles in 3 stations in the vicinity of the main cities, in order to estimate the concentration of trace elements (Rare Earth Elements) (Figure 49). Samples analysis was planned to take place during an ad hoc training course, however, due to technical reasons related to the availability of the laboratory equipment, the samples could not be processed and no result is available.

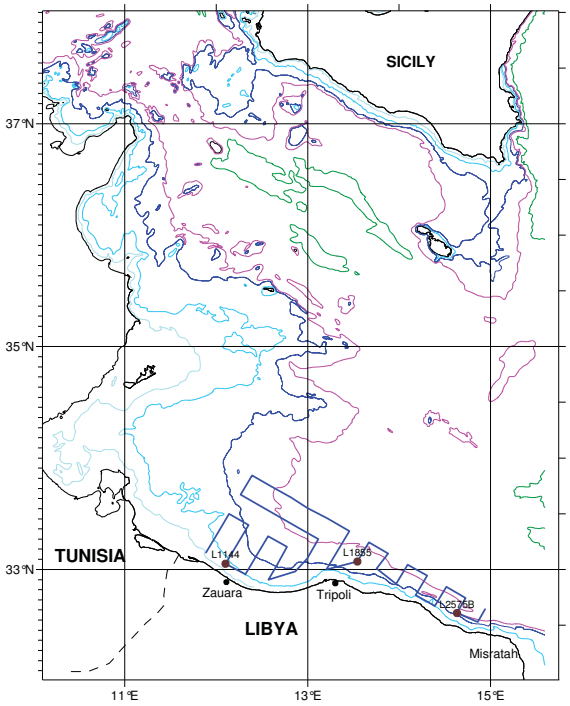

Figure 49. **Position of stations where samples of water were collected for the Rare Earth Elements analysis.**

10 Meteorology

Meteorological parameters were collected with an Andera meteo station. The station was used only during 5 days because of bad weather conditions. It collected data on wind direction and velocity with a Gill sonic anemometer, humidity anomalies with a Lyman Alpha high frequency humidity sensor, temperature and humidity with a thermo-hygrometer of the Vaisala Instruments. Data were recorded continuously 24 h a day.

Atmospheric data were collected with a Sodar (SOund Detection And Ranging) (Figure 50). The use of the tri-axial monostatic sodar (remote sensing instrument) will allow monitoring the evolution of the lowest atmospheric layers (up to 600m).

During part of the survey, data on air temperature and humidity, wind direction and velocity and height of inversion layers (layers of atmosphere with highest gradients of temperature) were collected at high temporal resolution, in view of estimating air-sea energy fluxes. Data were collected continuously, 24h a day.

Meteorological and atmospheric data will be post-processed to estimate wind velocity profiles in these atmospheric layers.

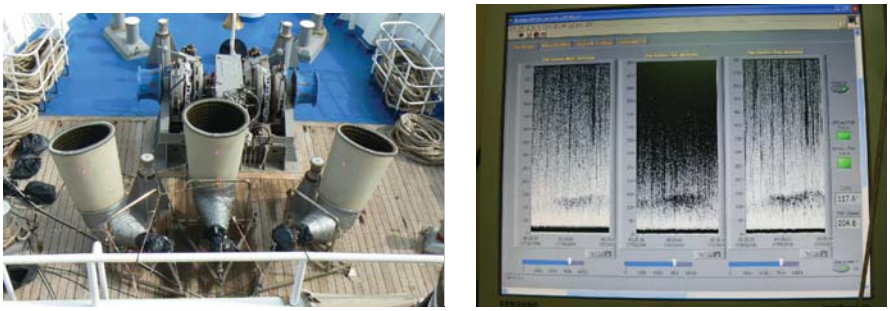

Figure 50. **Sodar (left) and sodar fax screen (right) showing intensity of the echo recorded by the detector layers of the atmosphere with highest gradients of temperature (inversion layers).**

11 References

Aminot, A., and Chaussepied, M. 1983. Manuel des analyses chimiques en milieu marin. Brest, CNEXO (Centre National pour l'Exploration des Océans): 395 pp.

Béranger, K., Mortier, L., Crepon, M. 2005. Seasonal variability of water transport through the Straits of Gibraltar, Sicily and Corsica, derived from a high-resolution model of the Mediterranean circulation. *Progress in Oceanography* 66 (2-4), 341-364.

Brassell, S.C., Eglinton, G., Marlowe, I.T., Pflaumann, U., Sarnthein, M. 1986. Molecular stratigraphy: a new tool for climatic assessment. *Nature*, 320: 129-133.

Charlson, R.J., Lovelock, J.E., Andreae, M.O. Warren, S.G. 1987. Oceanic phytoplankton, atmospheric sulphur, cloud albedo and climate. *Nature*, 326: 655-661.

Cros, L., Fortuño, J.-M. 2002. Atlas of Northwestern Mediterranean Coccolithophores. *Scientia Marina*, 66 (Suppl 1): 7-182.

Flagg, C.N., Smith, S.L. 1989. On the use of the acoustic Doppler current profiler to measure zooplankton abundance. *Deep-Sea Research*, 36: 455-474.

Folk, R.L. 1974. Petrology of Sedimentary Rocks. Hemp Hill, Texas, 182 pp.

Gontcharov, S., Calise, L., Knutsen, T., Van der Meeren, T., Angotzi, A.R., Bonanno, A., Patti, B., Mazzola, S., Buscaino, G. 2002. Target Strength and swimming behavior of herring larvae studied by the Split Beam Tracking Method. 6th ICES SYMPOSIUM "Acoustics in fisheries and aquatic ecology", 10-14 June 2002-Montpellier, France.

Greenlaw, C.F. 1979. Acoustical estimation of zooplankton populations. *Limnology and Oceanography*, 24: 226-242.

Guibout, P. 1987. Atlas hydrologique de la Méditerranée, Ifremer et S.H.O.M., Brest, 150 pp.

Holligan, P.M., Fernandez, E., Aiken, J., Balch, W.M., Boyd, P., Burkill, P.H., Finch, M., Groom, S.B., Malin, G., Muller, K., Purdie, D.A., Robinson, C., Trees, C.C., Turner, S.M., van der Wal, P. 1993. A biogeochemical study of the coccolithophore *Emiliania huxleyi* in the North Atlantic. *Global Biogeochemical Cycles*, 7: 879-900.

Honjo, S. 1976. Coccoliths: production, transportation and sedimentation. *Marine Micropaleontology*, 1: 65-79.

Iseki, K., MacDonald, R.W., Carmack, E. 1987. Distribution of particulate matter in the south-eastern Beaufort Sea in late summer. *Proc. NIPR Symposium of Polar Biology* 1: 35-46.

Keller, M.D., Bellows, W.K., Guillard, R.R.L. 1989. Dimethyl sulfide production in marine phytoplankton. In: E.S. Saltzman and W.J. Cooper (eds.), *Biogenic sulfur in the environment*, pp. 183-200. American Chemical Society, Washington.

Lacombe, H., Gascard, J.C., Gonella, J., Bethoux, J.-P. 1981. Response of the Mediterranean to the water and energy fluxes across its surface, on seasonal and interannual scales, *Oceanologica Acta*, 4(2): 247-255.

Lovegrove, T. 1966. The determination of dry weight of plankton and the effect of various factors on the values obtained. *In*: Some contemporary studies in marine science, pp. 462-467. Ed. by H. BARNES. London: Allen and Unwin Ltd.

MacLennan David, N., Simmonds, E.J. 1991. Fisheries Acoustics. Published by Chapman & Hall, 2-6 Boundary Row, London, pp. 201-280.

Malin, G., Kirst, G.O. 1997. Algal production of dimethyl sulphide and its atmospheric role. *Journal of Phycology*, 33: 889-896.

Ovchinnikov, I.M. 1966. Circulation in the surface and intermediate layers of the Mediterranean, *Oceanology* 24: 168-173.

Simó, R., Pedrós-Alió, C. 1999. Role of vertical mixing in controlling the oceanic production of dimethyl sulphide. *Nature*, 402: 396-399.

Stanton, T.K. 1989. Simple approximate formulas for backscattering of sound by spherical and elongated objects. *Journal of the Acoustic Society of America*, 86 (4), pp. 1499-1510.

Strickland, J.D.H., and Parsons, T.R. 1972. A practical handbook of seawater analysis. *Bulletin Fisheries Research Board of Canada*, 167: 1-311.

Swartzman, G., Brodeur, R., Napp, J., Hunt, G., Demer, D., Hewitt, R. 1999. Spatial proximity of age-0 walleye Pollock (*Theragra chalcogramma*) to xooplankton near the Pribilof Islands, Bering Sea, Alaska. *ICES Journal of Marine Science*, 56: 545-560.

Tufail, A. 1981. Identification sheets of phytoplankton species in Libyan coastal waters. *Bulletin of the Marine Biology Research Centre Tripoli Libya*, 2: 15-77.

UNESCO. 1968. Monographs on oceanographic methodology 2. Zooplankton sampling. Paris. 174 pp.

Visbeck, M. 2002. Deep velocity profiling using lowered acoustic Doppler current profilers: Bottom track and inverse solutions. *Journal Of Atmospheric and Oceanic Technology* 19 (5): 794-807.

Volkmen, J.K., Eglinton, G., Corner, E.D.S., Forsberg, T.E.V. 1980. Long-chain alkenes and alkenones in the marine coccolithophorid *Emiliania huxleyi*. *Phytochemistry*, 19: 2619-2622.

Westbroek, P. 1991. Life as a geological force. *Dynamics of the Earth*. Norton, New York.

Westbroek, P., van Hinte, J.E., Brummer, G.-J., Veldhuis, M., Brownlee, C., Green, J.C., Harris, R., Heimdal, B.R. 1994. *Emiliania huxleyi* as a key to biosphere-geosphere interactions. In: J.C. Green and B.S.C. Leadbeater (eds.), *The Haptophyte Algae*, *Systematics Association Special Volume* 51, 321-334. Clarendon Press, Oxford.

Wüst, G. 1961. On the vertical circulation of the Mediterranean Sea, *Journal of Geophysical Research*, 66: 3261-3271.

Zorgani, M.E. 1982. Qualitative and quantitative zooplankton in the Gulf of Gabes and adjacent Libyan waters. *Bulletin of the Marine Research Centre of Tripoli Libya* 3: 1-22.

FAO MEDSUDMED PROJECT
Food and Agriculture Organization of the United Nations (FAO)
Fisheries and Aquaculture Department
Viale delle Terme di Caracalla
00153 Rome, Italy
Tel.: +39 06 570 54492 - Fax: +39 06 570 55188
email: medsudmed@fao.org
URL: http://www.faomedsudmed.org

ITALIAN MINISTRY OF AGRICULTURE, FOOD AND FORESTRY POLICIES

Ministero delle Politiche Agricole Alimentari e Forestali
Viale dell'Arte 16
00144 Roma, Italia
URL: http://www.politicheagricole.it

Regione Siciliana

Regione Siciliana
Via degli Emiri n. 45,
90135 Palermo, Italia
URL: http://pti.regione.sicilia.it